Jour. Geol. Soc. India (2022) 98:245-259
https://doi.org/10.1007/s12594-022-1965-6

ORIGINAL ARTICLE

Mineral Chemistry and Geothermometry of Biotite in the Granitoids, Located in and around Jirang-Patharkhamah Area, Ri-Bhoi District, Meghalaya, India

Anamika Gogoi[1,*] and Balen Bhagabaty[2]

[1]Department of Geology, Cotton University, Guwahati - 781 001, India
[2]Department of Geological Sciences, Gauhati University, Guwahati - 781 014, India
***E-mail:** ganamika1234@gmail.com*

Received: 25 March 2020 / Revised form Accepted: 7 June 2021

ABSTRACT

Granitoids are well exposed in Jirang-Patharkhamah area (latitude N 25°57'- 25°41' and longitude E 91°30' - 91°38'). The area lies mostly inRi-Bhoidistrict and is also extended to West Khasi Hills district of Meghalaya. The granitoids are medium grained and nonporphyritic. The colour is dominantly grey although some granitoids are pink in colour. The common minerals in order of abundance are quartz, plagioclase, K-feldspar, biotite and hornblende. Secondary minerals are sericite, chlorite, muscovite, secondary hornblende and secondary biotite. Among accessory minerals, sphene, zircon, apatite, calcite, zoisite, magnetite and monazite are significant. The intergrowth textures such as perthite, myrmekite in these rocks indicate that the rocks were affected by low temperature alteration. The representative samples ploy in the field of granite in various geochemical discrimination diagrams. The aim of the present paper is geochemical characterisation of the granitoids using major and trace elements (including REE). The whole rock geochemistry reveals that the granitoid is I-type, calc-alkaline, metaluminous to weakly peraluminous and an attempt is made to examine the nature of the magma based on biotite mineral chemistry. The biotite chemistry indicates that the granitoid is I-type and calc-alkaline. The paper also aims to estimate temperature of emplacement of granitoids based on two feldspar geothermometer and Ti-in biotite geothermometer. The temperature calculated from two feldspar thermometry is in the range 512-602°C and the average is 550°C. The temperature calculated by Ti-in biotite thermometer is in the range 623 to 656°C and the average is 645°C. Geothermometric results plays an important role in definition of petrogenetic history and regional tectonism.

INTRODUCTION

The Shillong plateau is characterised by the presence of a number of granitic bodies, e.g., Mylliem granite, South Khasi batholith, Kyrdem granite and Nongpoh granite. In recent past detailed geological and geochemical studies on granitoids of Shillong plateau have been carried out by many workers e.g., Ghosh et al. (1991, 1994a, 2005), Kumar et al. (1990, 1998, 2005, 2017), Ray et al. (2011). The study area is located in Shillong plateau and available geoscientific data of the area is scanty and geochemistry, mineral chemistry data is almost absent. The Shillong plateau constitutes the leading edge of the Indian plate during its supposed oblique collision with the Australo-Antarctic plate at ca.650-500Ma. Thus, an appraisal of the thermal events in the plateau can offer clues regarding its role in Pan Gondwana reconstruction. The area lies mostly in Ri-Bhoi district and is also extended to West Khasi hills district of Meghalaya. Location map of the area is given in Fig.1.

Igneous rocks, mainly granitoids, constitute one of the most essential parts of the continental crust. They usually form by partial melting or assimilation-fractional crystallisation (AFC) processes in the lower crust and are subsequently intruded into the middle or upper crust. By doing so, they dramatically influence the complete continental crust with respect to, for instance, rheology and geochemistry. Understanding the evolution of continental crust, therefore, demands comprehension of granitoid's origin and petrogenesis. Therefore, study of granitic rocks based on whole rock geochemistry and a parallel study on mineral chemistry can contribute a lot in understanding the evolution of the continental crust. Biotite composition is a valuable guide to granite petrogenesis (Dodge et al., 1969; Neiva, 1981; Spear, 1981; Finch et al., 1995). Biotite is the reservoir of excess aluminium in granitic rocks in the absence of garnet, cordierite, or Al_2SiO_5 polymorphs. Therefore, biotite is an important aluminium concentrator and it reflects the peraluminosity of the host magma (Shabani et al., 2003). Wones and Eugster (1965) established biotite as a valuable indicator of oxidation-reduction conditions in granitic magmas.

A number of geothermometers are applied to granitic rocks (Anderson et al., 2008). The thermometers are based on experimental calibrations and can carry significant uncertainty. Plutons serve as crustal "nails" and geothermometry can be used in study of these plutons (Anderson et al., 1988). Geothermometry plays an important role in defining the petrogenetic history and regional tectonism.

The chemical composition of different minerals helps to understand the various igneous processes involved during the formation of the mineral. Composition of ferromagnesian minerals like amphibole and biotite reflect the whole rock composition and origin of granitoids. Biotite has the potential to reflect both the nature and the physico-chemical conditions of the magma from which it formed (Ague and Brimhall,1988; Shabani et al.,2003).

The present paper is documentation of part of the study on granitoids of Jirang-Patharkhamaharea (latitude N 25°57'- 25°41' and longitude E 91°30' - 91°38') of Ri-Bhoi district, Meghalaya. This paper highlights field, petrographic, geochemical, mineral, chemical

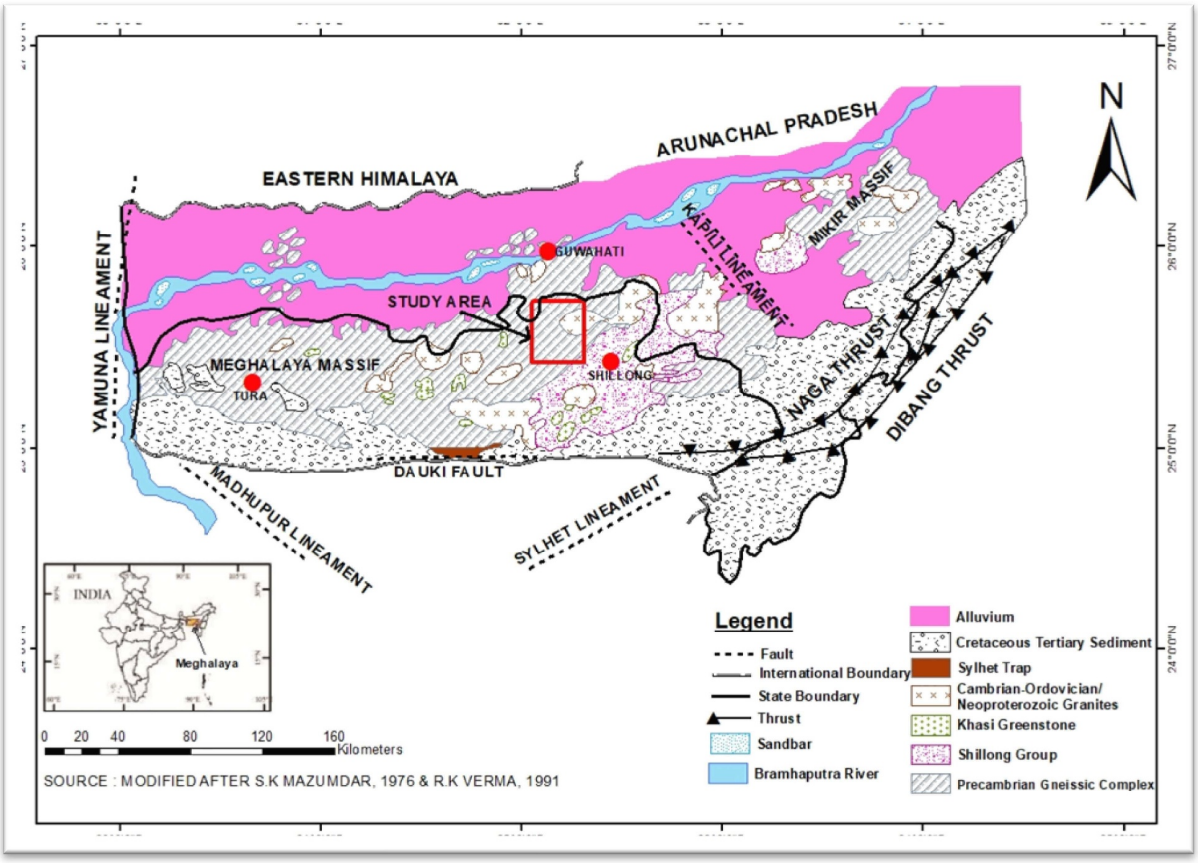

Fig.1. Geological map of the Shillong Plateau showing the location of study area (modified after Mazumdar,1976)

and geothermometric studies of the granitoid occurring in the area.

GEOLOGICAL SETTING

Regional Geology

The study area is situated in the central part of the gneissic complex of the Shillong plateau which was believed to be north-eastern extension of the Peninsular shield of India (Evans, 1964). The plateau encompasses parts of Meghalaya, adjoining hilly tracts of Goalpara and Kamrup districts of western Assam and the hilly tracts of the Karbi Anglong district (Mikir Hills). The plateau is separated from Peninsular India by Garo Rajmahal gap.

The Precambrian rocks of the Plateau are sub-divided into the gneissic complex, non-porphyritic granites, the Shillong Group of supracrustal rocks, the Khasi greenstone and porphyritic plutons. The gneissic complex and the non-porphyritic granites form the basement for the Shillong Group. The Paleoproterozoic gneissic complex acts as the basement of the Shillong Plateau (Mazumdar, 1976) and overlain by metasedimentary and metavolcanics of Shillong Group and metadolerite (Khasi greenstone). An assortment of rock types including sillimanite-bearing gneisses, amphibolites, banded iron formations, granulites and granite gneisses, collectively known as the Gneissic Complex (Mazumdar, 1976, 1986). Most part of the Shillong plateau is constituted by basement gneisses and Shillong Group of rocks. A number of felsic plutons occur in different parts of Shillong Plateau. South Khasi batholith, Mylliem granite, Nongpoh granite, Kyrdem granite are such plutons. The Mylliem granite and South Khasi batholiths are intrusive into the Shillong Group of rocks. The Nongpoh and South Khasi batholiths are intrusive into the Shillong Group as well as basement gneissic complex. The southern part of the plateau is covered by Cretaceous Sylhet basalts and the Tertiary shelf sediments. The Shillong Group of rocks, occurs in a 240 kilometres long NE-SW trending intracratonic basin (from Jadukata river section in southern Meghalaya to north of Mikir hills in central Assam) (Mitra, 2005), was metamorphosed to greenschist facies and rests unconformably marked by a basal conglomerate (Nandy, 2001).

The basic granulites and metapelitic granulites occur as patches within the rocks of gneissic complex in Sonapahar area of Shillong plateau (Lal et al., 1978; Chatterjee et al., 2007), Garo-Goalpara hills (Chatterjee et al., 2007; Bhagabaty and Mazumdar, 2008) and Patharkhang (Dwivedi and Theunuo, 2011). The gneissic complex rocks of Shillong plateau are of Mesoproterozoic age 1596 ± 19 Ma (Chatterjee et al., 2007), 1150 – 1714 Ma (Ghosh et al., 2005), U-Pb zircon age of ca 1600 Ma (Yin et al., 2010a) and 1415 - 1451 Ma from Riangdo gneiss (Bidyananda and Deomurari, 2007). The basement rocks of Shillong plateau are intruded by different phases of granitoids (Mazumdar, 1976, 1986). The granitoids has younger ages from south-west to north-east (Kumar, 1998). Their age ranges from 479 to 881 Ma (Ghosh et al., 1991; 1994a; 2005). The xenoliths of both metasediments and mafic rocks belonging to Shillong Group are reported from Mylliem granitoids (Ray et al., 2011). The Sung valley ultramafic–alkaline–carbonatite complex of early Cretaceous age is one of the several alkaline intrusions that occur in the Shillong plateau. A temporal link to the Kerguelen plume with Sung valley support by the U–Pb age of perovskite (115 ± 5.1 Ma) from ijolite (Srivastava et al., 2005). However, Chatterjee et al. (2011) determined EPMA age of monazite (1609±09 Ma) for the high grade metapelites from the Garo-Goalpara area. The Rongjeng granite gneiss record the oldest magmatic events at 1778±37 Ma whereas an inherited zircon core with an age of 2566.4±26.9 Ma, indicates the presence of recycled Neoarchean crust in the basement granite gneisses (Kumar et al., 2017). The occurrence of A-type granite plutons has been recognized in the Dizo valley of the Karbi hills, these Kathalguri granites have been dated as ~515 Ma (Majumdar and Dutta, 2016).

Four generations of folding have been described in the Shillong Group metasedimentary units. The earliest structures are very tight to isoclinal folding (F_1) on bedding plane (S_o). These folds have high amplitude to wave length ratio, with a pervasive axial planar cleavage (S_1). They have been affected by coaxial, open to tight upright folds (F_2) with axial plane striking NNE, with the development of crenulation cleavage (S_2). Both F_1 and F_2 folds provide evidence of buckling origin. In the more schistose rocks, NE-trending open recumbent fold (F_3), affecting F_1 cleavage and F_2 axial planes, represent structures of the third generation. The latest structures are upright conjugate folds and kink bands (F_4) with axial planes striking NE, EW and chevron folds with NW striking axial planes. The structure of the last generation, therefore, provides evidence of longitudinal shortening of the Shillong Group of rocks (Mitra, 1998).

Geology of the Area

An attempt is made here to indicate the inter-relationship of the different rock types of the area. The area under study is a part of large basement gneissic complex of Shillong plateau.The first geological map of the area was published by Dash and Chatterjee (1992). A modified geological map representing different litho units including newly identified diorites are shown in Fig.2.

The rocks are of Precambrian to Cambrian age mainly comprising quartzo-feldspathic gneisses (QFG), granitoids, amphibolites, diorites (metasomatised), metapelites, calc-silicate rocks and iron formations.The granitoid is one of the most dominant rock types of the area. The rocks are medium grained and massive. The rocks exhibit contact relationship with quartzo-feldspathic gneiss (Fig.3A). The amphibolites are showing sharp contact relationship with the granitoid (Fig.3B). The diorites are scattered mainly in the southern part of the study area.There are many feldspar bearing veins within the diorites (Fig.3C). These later intrusive feldspar veins are connected to neighbouring granitoids. Pegmatitic vein is found in granitoids (Fig.3D). Quartzo-feldspathic gneisses are the common rock types in the entire study area. At certain places, the quartzo-feldspathic gneisses grade into migmatites with well-defined biotite rich melanosomes and granitic leucosomes. Flow folding in migmatites is observed (Fig.3E). Atplaces quartzo-feldspathic gneisses are well foliated. Folding in quartzo-feldspathic gneiss is found at some places (Fig.3F). Co-folded bands of amphibolites with quartz-feldspathic gneisses are observed in certain places.

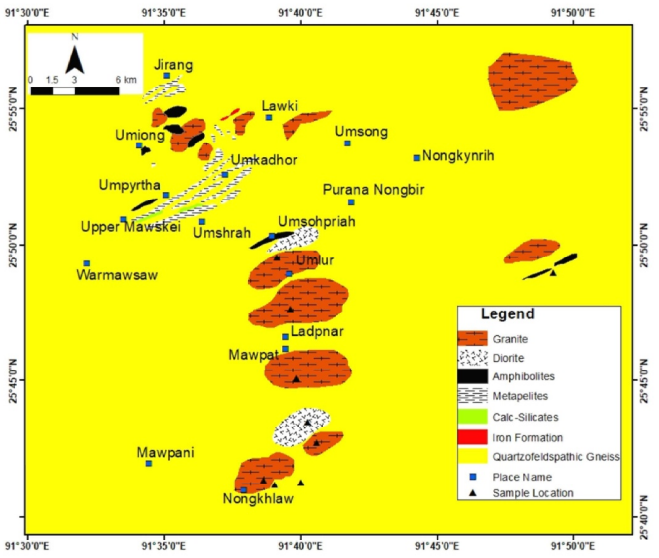

Fig.2. Geological map of the study area (modified after Dash and Chatterjee, 1992).

The less frequently observed other rock types in the area includes calc-silicate gneiss, cordierite-sillimanite bearing metapelites and iron formations. Calc-silicate gneisses are strongly associated with amphibolites and metapelites. At places, calc-silicate gneisses and amphibolites are so closely associated that they can be expected in a single exposure. The cordierite–sillimanite bearing gneisses represent the metapelitic rocks in the area. Iron formations are found together with the bands of quartzo-feldspathic gneisses.

PROCEDURE AND ANALYTICAL PROTOCOL FOR THE WORK

Standard procedures were adapted for making thin sections. The thin sections were prepared for the petrographic study and mineral chemistry. For EPMA selected sections were polished using chromium powder and diamond paste. Electron probe micro analyses of different mineral phases were performed with Cameca SX100 EPMA instrument, at IIT Kharagpur. The major oxide analyses were done by using Siemens SRS-3000 X-ray fluorescence (XRF) spectrometers at Wadia Institute of Himalayan Geology, Dehradun. Trace elements were analysed by ICP-MS technique through Perkin Elmer SCIX ELAN DRC-E instrument at Wadia institute of Himalayan Geology.

RESULTS

Petrography

The rock exhibit medium grained hypidiomorphic texture in thin section and common minerals in order of abundance are quartz, plagioclase, k-feldspar, biotite and hornblende. Secondary minerals are sericite, chlorite, muscovite, secondary hornblende and secondary biotite. Among accessory minerals, sphene, zircon and apatite, calcite, zoisite, magnetite and monazite are significant assemblages:

1) Quartz + plagioclase + K- feldspar + biotite +sphene + opaque phases ± zircon ± monazite ± apatite ± zoisite ± (sec sericite + sec muscovite + sec chlorite)
2) Quartz +plagioclase +hornblende +K-feldspar + biotite +sphene ± clinopyroxene ±opaque phases ± zircon ± zoisite ± allanite ± (sec sericite + sec muscovite ± sec chlorite± sec hornblende ± sec biotite)

The rocks are showing distinctive two feldspar mineralogy (Fig.4A). Hornblende is present (Fig.4B) in some of the thin sections and biotite is commonly present (Fig.4C). Presence of hornblende, biotite and sphene and absence of primary muscovite supports metaluminous character of the rock. Zircon, apatite are euhedral to subhedral (Fig.4C),supporting I-type character. Predominance of sphene (Fig.4C) supports I-type character. Presence of allanite supports the involvement of lower crustal component. Texturally, two types of hornblende are observed. The primary hornblendes are dominantly coarse grained, subhedral, prismatic and characterised by yellowish to green pleochroism (Fig.4B). The secondary hornblendes are bluish green and irregular mass stabilised along the border/fracture of clino-pyroxene (Fig.4D). Intergrowth textures like perthite, myrmekite are present in these rocks indicating low temperature alteration (Fig.4E, F).

The sequence of crystallisation can be interpreted from texture of the rock. The accessory minerals like zircon, apatite are formed first and followed by crystallisation of plagioclase, followed by clino-pyroxene. Then hornblende and biotite were crystallised. Secondary hornblende, muscovite, biotite and chlorite were formed during cooling of the pluton in H_2O rich environment.

Whole Rock Geochemistry

The major elemental analyses are presented in Table 1. The rocks have high SiO_2 contents, varying from (70.35 - 77.42 wt%), $Fe_2O_3^t$

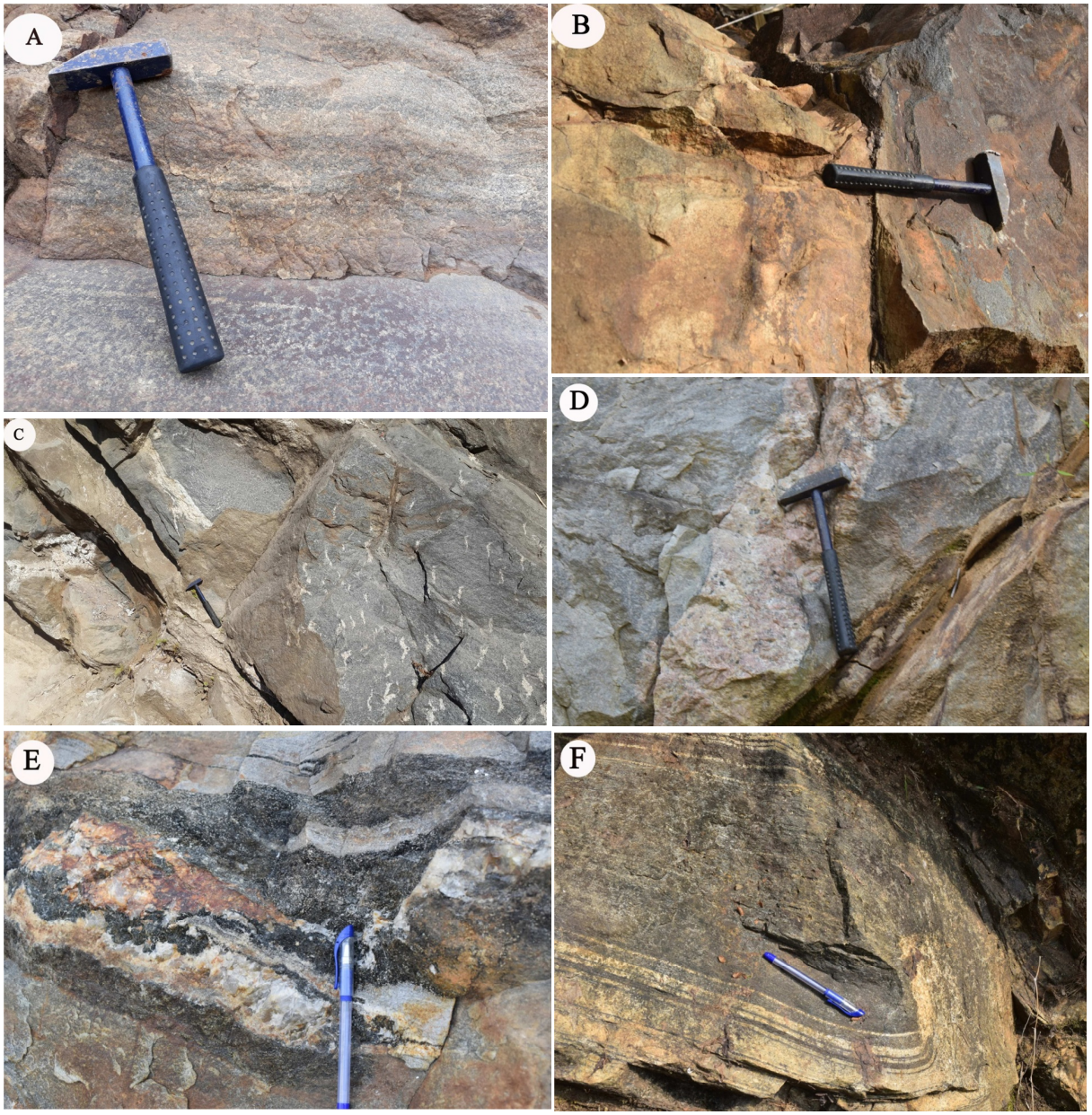

Fig.3. **(A)** Contact between granitoid and Quartzo-feldspathic gneiss. **(B)** Contact between granitoid and amphibolites. **(C)** Contact between diorite and quartzofeldspathic gneiss, there are lots of feldspar bearing veins within diorite. **(D)** Pegamtite vein within granitoid. **(E)** Migmatite. **(F)** Fold in quartzo-feldspathic gneiss.

(1.27 - 3.11wt%), MgO (0.06 - 0.52 wt%), CaO (0.69 - 1.87 wt%), Na_2O (3.44 - 4.84 wt%), K_2O (2.08 - 5.25 wt%) and TiO_2 (0.09 - 0.39 wt%). Al_2O_3, TiO_2, MnO, MgO, Fe_2O_3, CaO, K_2O, P_2O_5 show negative correlation with respect to SiO_2. Na_2O showing positive correlation with respect to SiO_2. Total alkali values ranges from 7.22 to 9.08 wt%. K_2O/Na_2O ratios vary from 0.40 to 1.52. Different representative discrimination diagrams indicate that the present granitoid is granite (Fig.5, 6). The present granitoids are calc-alkaline nature and are found to be of I-type (Fig.7). The A/CNK < 1.1, indicates metaluminous to weakly peraluminous nature (Fig.8). I-type calc-alkaline granitoids can be formed from melting of lower crust, fractional crystallisation of mafic magmas derived from mantle, or mixing of mantle derived magmas and continental felsic melts (Kemp et al., 2007). Calc-alkaline, I-type, acidic composition indicates crustal participation in magma generation (Egal et al., 2002). The present granitoid is iron rich (Fig.9).

Trace element data are presented in Table 2. The trace elements Ba, Eu, Tb, Dy, Ho, Er, Tm, Yb, Lu, Y show a positive trend with SiO_2 while Rb, Sr, Zr, Nb, Zn, Cr, La, Ce, Pr, Nd, V, Sc, Ga, Th show a negative trend with SiO_2 concentration. The high field strength elements like Nb, Zr, La, Th shows negative correlation with Y and show positive correlation with increasing abundance of SiO_2. The large ion lithophile (LIL) elements Ba, Rb show positive correlation with increasing concentration of SiO_2 and Sr shows negative correlation with increasing concentration of SiO_2. In the primitive mantle normalised multi-element spider diagram (values of normalisation after Sun and McDonough,1989) Ba, Nb, Sr, P, Ti, Yb are showing depleted trendand alsoindicating relative enrichment in Th, U, K (Fig.10).

The rare earth element (REE) values for granitoids are shown in Table 3. The $(La/Yb)_N$ is high (5.58 to 67.78, average 12.95) indicating a high degree of LREE and HREE fractionation. The $(La/Sm)_N$ (2.66 to 5.77, average 3.78) is indicating fractionation of LREE.$(Tb/Yb)_N$ (0.87 to 4.64, average 1.77) which in turn reflects the degree of HREE fractionation. The chondrite normalised REE value plot is shown in Fig.11. Normalisation factors were used from Taylor and McLennan

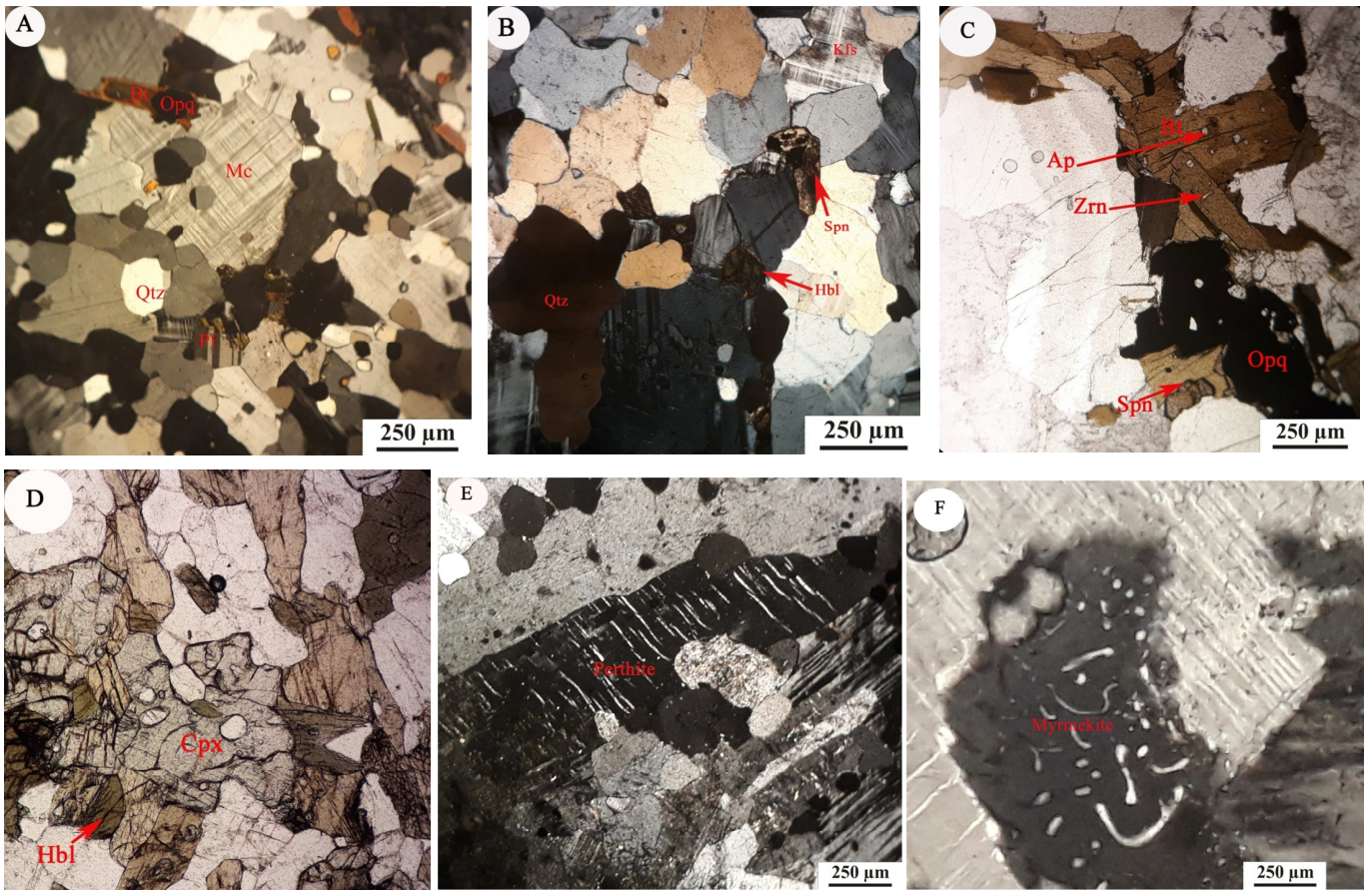

Fig.4. (A) Plagioclase, microcline, quartz, biotite, and opaque in granitoid. **(B)** Hornblende, sphene, K-feldspar, quartz in granitoid. **(C)** Inclusion of apatite and zircon in biotite; opaque is inclose association with sphene in granitoid. **(D)** Pseudomorphous replacement of clinopyroxene by hornblende in granitoid. **(E)** Perthite in granitoid. **(F)** Myrmekite in granitoid

(1985). The Eu anomaly (Eu/Eu*) is negative (0.21 to 0.48, average 0.34) suggesting strong plagioclase fractionation.

Mineral Chemistry

Biotite

The EPMA data of biotite (14 data points) are presented in Table 4(a). Structural formulae of biotite were calculated on the basis of 11 oxygens using Excel Spreadsheet version for biotite formula calculation. The biotites in granitoid show variation in SiO_2 content from 34.90 to 36.58 wt%. The X_{Fe} value varies from 0.59 to 0.63 (average 0.62). X_{Mg} values vary from 0.38 to 0.41 (average 0.39). Thebiotitesare iron rich (X_{Fe}> 0.5).

In the FeO*-MgO-Al_2O_3 diagram of Abdel–Rahman (1994), the biotite compositions for present granitiod rocks distributed between alkaline and calc-alkline fields (Fig.12). The variables total Al and Fe/(Fe+Mg) are commonly used to display compositional relationships of tri-octahedral micas from igneous suite (Speer,1984). The composition of granitic rocks is plotted in the annite – siderophyllite – phlogopite - eastonite (ASPE) quadrilateral (Fig. 13). The biotites are fairly rich in iron and the Fe/(Fe+Mg) ratio varies from 0.59 to 0.62 apfu. According to the nomenclature of Deer et al. (1986), the biotite of the granitoid is identified as annite - siderophyllitic (Fig.14). According to classification diagram of Deer et al. (1986) the biotites of the granitic rocks are classified as Fe rich biotite (Fig.15). The biotites have high Al_2O_3 (varies from13.42 to 16.62 wt%, average 15.22 wt %) and low TiO_2 value (vary from 2.25 to 2.68 wt %, average 2.51 wt%) reflecting the characteristic of ilmenite series of granitoids. Biotite with high aluminium concentration is characteristic of peraluminous granite (Clarke et al., 2005; Dahlquist et al., 2007). The Ti content in the biotite is low (vary from 0.13 to 0.29 apfu, average 0.29 apfu). The Ti content in biotite is dependent on temperature of crystallisation of biotite and oxygen fugacity (fO_2) (Henry et al., 2005). Low Ti content correlates with the low temperature of crystallisation (Henry et al., 2005). Abdel –Rahman's (1994) diagrams for identifying magmatic nature based on biotite chemistry are indicating calc-alkaline nature of the granitoids (Fig.16a, b).

K-feldspar

The analytical data of K-feldspar are presented in Table 5(a). The SiO_2 content varies from 63.83 to 65.72 wt.%. CaO content varies from 0.00 to 0.07 wt.%. Na_2O varies from 0.32 to 0.98 wt.%. BaO varies from 0.17 to 0.33 wt.%. The orthoclase component varies widely, from 75.16 to 96.91 mole percent. Anorthite content is low, up to 0.00 to 0.33 mole percent. The albite (Ab) component varies from 3.09 to 24.51 mole percent.

Plagioclase

The EPMA data of plagioclases along with structural formula are presented in Table 5(b). The SiO_2 content varies from 63.57 to 69.44 wt.%. The Al_2O_3 content varies from 19.64 to 23.07 wt.%. CaO content varies from 0.49 to 4.35 wt.%, Na_2O content varies from 9.43 to 11.58 wt.%. K_2O varies from 0.12 to 0.27 wt.%. FeO content varies from 0 to 0.13wt.%. BaO content varies from 0 to 0.08 wt.%. The anorthite (An) content varies from 2.26 to 20.03, albite (Ab) component varies from 78.78 to 96.85 mole percent, orthoclase (Or) component varies from 0.66 to 1.48 mole percent, thus indicating albitic plagioclase in the granitoids.

Table 1. Major oxide (wt %) data of granitoids.

	A1	A2	A3	A4	A5	A6	A7	A8	A9	A10	A11	A12	A13	A14	A15	A17	A18	A21	A23	A24	A28	A32	Avg.
SiO_2	76.93	76.09	74.59	76.28	76.23	76.12	74.26	75.31	75.04	77.42	70.35	75.53	74.85	73.29	72.57	75.18	74.89	76.20	72.46	75.02	73.16	73.12	74.77
TiO_2	0.15	0.16	0.11	0.15	0.18	0.20	0.19	0.16	0.20	0.14	0.39	0.09	0.19	0.16	0.20	0.19	0.20	0.22	0.20	0.18	0.16	0.18	0.11
Al_2O_3	12.31	12.43	14.12	12.52	12.25	12.79	13.50	13.17	12.88	12.34	14.59	13.58	13.31	14.41	14.62	12.81	12.95	12.38	14.59	12.68	14.11	13.94	13.04
$Fe_2O_3^t$	1.76	1.86	1.51	1.72	2.22	1.56	2.01	1.77	1.98	1.66	3.11	1.27	1.92	1.51	1.96	2.32	2.41	1.89	1.87	2.71	1.62	1.74	1.93
MnO	0.04	0.03	0.02	0.03	0.06	0.06	0.02	0.02	0.08	0.02	0.04	0.02	0.02	0.02	0.03	0.02	0.02	0.01	0.03	0.02	0.05	0.05	0.03
MgO	0.09	0.07	0.14	0.07	0.08	0.17	0.17	0.15	0.23	0.07	0.52	0.06	0.16	0.19	0.23	0.14	0.14	0.36	0.29	0.16	0.20	0.25	0.18
CaO	1.23	1.02	1.65	0.93	1.07	0.88	1.08	1.11	0.92	0.69	1.87	1.02	1.10	0.95	0.92	1.07	1.06	1.07	1.08	0.91	1.47	1.55	1.12
Na_2O	4.03	4.10	4.72	3.88	3.88	5.22	3.63	3.55	5.12	3.74	4.41	4.84	3.53	3.94	3.94	4.57	4.66	5.17	3.99	4.31	3.46	3.44	4.19
K_2O	3.27	3.43	2.66	3.90	3.34	2.27	4.76	4.69	2.50	4.17	3.21	3.65	4.81	5.14	5.13	3.24	3.15	2.08	4.88	3.41	5.25	4.97	3.81
P_2O_5	0.02	0.01	0.01	0.01	0.02	0.01	0.02	0.02	0.01	0.01	0.06	0.01	0.02	0.05	0.05	0.02	0.02	0.02	0.06	0.02	0.04	0.04	0.03
K_2O+Na_2O	7.30	7.53	7.38	7.78	7.22	7.49	8.39	8.24	7.62	7.91	7.62	8.49	8.39	9.08	9.07	7.81	7.81	7.25	8.87	7.72	8.71	8.41	8.00
K_2O/Na_2O	0.81	0.84	0.56	1.01	0.86	0.43	1.31	1.32	0.49	1.11	0.73	0.75	1.36	1.30	1.30	0.71	0.68	0.40	1.22	0.79	1.52	1.44	0.95
Na_2O/K_2O	1.23	1.20	1.77	0.99	1.16	2.30	0.76	0.76	2.05	0.90	1.37	1.33	0.73	0.77	0.77	1.41	1.48	2.49	0.82	1.26	0.66	0.69	1.22
A/NK	1.21	1.19	1.33	1.88	1.23	1.16	1.21	1.21	1.16	1.16	1.36	1.14	1.21	1.20	1.21	1.16	1.17	1.15	1.23	1.18	1.24	1.26	1.24
A/CNK	0.99	1.01	1.03	1.02	1.03	1.01	1.03	1.02	1.01	1.04	1.03	0.99	1.02	1.05	1.07	0.99	1.00	0.97	1.06	1.02	1.00	1.01	1.02

Table 2. Trace element data (in ppm) of granitoids

	A1	A2	A3	A4	A5	A6	A7	A8	9A	10A	11A	12A	A13	A14	A15	A17	A18	A21	A23	A24	A28	A32
Ba	1269.00	1184.00	981.00	1280.00	1065.00	912.00	700.00	751.00	1284.00	1273.00	1443.00	1119.00	772.00	492.00	521.00	981.00	957.00	941.00	545.00	939.00	532.00	489.00
Rb	76.00	73.00	33.00	85.00	89.00	41.00	191.00	177.00	53.00	94.00	78.00	86.00	189.00	190.00	194.00	75.00	74.00	47.00	185.00	82.00	310.00	286.00
Sr	87.00	71.00	96.00	73.00	82.00	58.00	24.00	25.00	57.00	53.00	155.00	64.00	25.00	109.00	108.00	58.00	58.00	89.00	121.00	56.00	95.00	100.00
Zr	257.00	248.00	135.00	262.00	269.00	213.00	208.00	191.00	222.00	221.00	562.00	139.00	199.00	165.00	190.00	294.00	308.00	325.00	201.00	275.00	149.00	164.00
Nb	6.00	8.00	5.00	6.00	7.00	10.00	19.00	15.00	12.00	3.00	9.00	3.00	16.00	9.00	10.00	10.00	10.00	12.00	11.00	8.00	25.00	20.00
Co	133.00	83.00	71.00	40.00	48.00	38.00	69.00	59.00	35.00	48.00	45.00	67.00	54.00	46.00	94.00	56.00	52.00	46.00	43.00	53.00	44.00	40.00
Zn	32.00	24.00	23.00	26.00	58.00	121.00	16.00	14.00	54.00	30.00	40.00	24.00	16.00	35.00	39.00	16.00	15.00	10.00	43.00	19.00	33.00	33.00
Cr	8.00	9.00	8.00	10.00	6.00	11.00	9.00	9.00	11.00	8.00	11.00	7.00	8.00	10.00	8.00	8.00	10.00	7.00	9.00	9.00	7.00	9.00
Y	38.00	37.00	22.00	35.00	40.00	33.00	60.00	58.00	18.00	35.00	27.00	22.00	59.00	32.00	32.00	44.00	44.00	45.00	29.00	43.00	55.00	44.00
V	6.00	4.00	7.00	5.00	6.00	8.00	9.00	8.00	9.00	5.00	30.00	7.00	9.00	9.00	13.00	6.00	11.00	8.00	15.00	7.00	11.00	17.00
Sc	5.30	5.30	4.60	4.40	5.90	2.40	5.60	3.80	4.20	3.20	5.80	6.10	4.30	2.80	3.40	6.00	6.50	7.40	3.20	5.10	3.80	4.60
Cu	5.00	5.00	6.00	3.00	2.00	22.00	1.00	1.00	3.00	4.00	4.00	1.00	1.00	2.00	1.00	2.00	3.00	1.00	2.00	82.00	2.00	16.00
Ga	16.00	15.00	15.00	15.00	16.00	19.00	18.00	17.00	18.00	15.00	15.00	18.00	17.00	20.00	19.00	17.00	16.00	18.00	21.00	17.00	18.00	18.00
U	BDL	2.60	5.20	BDL	3.30	5.60	3.10	8.90	4.50	3.80	7.00	BDL	4.50	34.80	33.40	3.80	BDL	5.00	32.10	BDL	22.80	10.60
Th	13.00	13.00	24.00	16.00	16.00	23.00	32.00	41.00	17.00	16.00	159.00	11.00	34.00	85.00	91.00	14.00	12.00	25.00	99.00	14.00	59.00	53.00

Table 3. Rare earth element (ppm) data of granitoids

	A1	A2	A3	A4	A5	A6	A7	A8	9A	A10	A11	A12	13A	14A	15A	17A	A18	A21	A23	A24	A28	A32	Avg. (all)	
La	54.00	48.00	37.00	57.00	58.00	48.00	63.00	47.00	53.00	64.00	188.00	31.00	61.00	48.00	48.00	37.00	33.00	42.00	49.00	50.00	59.00	46.00	**55.50**	
Ce	114.00	103.00	70.00	118.00	124.00	97.00	127.00	92.00	111.00	135.00	383.00	65.00	122.00	90.00	92.00	81.00	63.00	89.00	93.00	111.00	122.00	92.00	**113.36**	
Pr	12.90	11.40	7.00	13.30	14.00	10.90	12.90	10.40	12.00	15.10	38.00	7.20	12.70	9.30	9.20	9.40	8.40	10.50	9.40	12.80	13.50	9.30	**12.25**	
Nd	53.60	47.90	27.00	54.50	58.70	42.80	49.80	39.30	46.70	61.70	133.00	29.10	48.70	34.30	33.40	39.60	35.50	42.90	33.90	52.50	44.00	33.10	**47.36**	**ΣAv.LREE=246**
Sm	10.99	9.77	5.03	10.57	12.08	8.36	10.20	8.86	9.25	12.21	20.50	5.60	9.49	6.43	6.40	8.71	7.79	9.30	5.95	12.00	8.07	6.17	**9.26**	
Eu	1.35	1.21	0.71	1.31	1.42	0.72	0.68	0.61	0.78	1.06	1.14	0.95	0.69	0.66	0.56	1.02	0.92	1.03	0.58	1.43	0.67	0.57	**0.91**	
Gd	9.36	8.42	4.14	8.85	10.49	6.30	9.79	8.31	6.93	9.83	15.40	4.61	9.10	5.14	5.00	8.04	6.95	8.30	4.51	10.45	7.68	4.98	**7.84**	
Tb	1.75	1.57	0.66	1.59	1.93	0.95	2.01	1.68	0.96	1.67	2.05	0.77	1.88	0.85	0.82	1.59	1.36	1.62	0.70	2.06	1.19	0.87	**1.39**	
Dy	12.60	11.11	4.26	11.05	13.81	5.13	16.20	13.79	4.96	11.38	10.00	5.02	14.40	5.60	5.21	12.11	10.10	11.94	4.29	14.88	7.01	6.19	**9.59**	
Ho	2.54	2.25	0.86	2.21	2.82	0.92	3.59	2.96	0.63	2.10	1.41	0.97	3.08	1.03	0.94	2.50	2.11	2.54	0.77	3.17	1.50	1.28	**42.18**	
Er	6.65	5.83	2.35	5.80	7.34	2.53	9.98	8.48	1.44	5.25	2.92	2.42	8.66	2.61	2.45	6.65	5.57	6.87	1.86	8.48	4.19	3.50	**5.08**	**ΣAv.HREE=83**
Tm	0.98	0.90	0.40	0.88	1.13	0.41	1.62	1.38	0.19	0.37	0.30	0.36	1.47	0.39	0.37	1.04	0.87	1.11	0.26	1.27	0.67	0.57	**0.77**	
Yb	6.52	6.00	3.22	5.81	7.93	3.21	11.69	9.92	1.33	4.69	1.87	2.45	9.91	2.66	2.37	7.06	5.86	7.66	1.76	8.89	2.37	2.37	**5.25**	
Lu	1.05	0.92	0.58	0.90	1.36	0.58	1.90	1.63	0.26	0.69	0.32	0.43	1.65	0.45	0.41	0.56	0.97	1.27	0.31	1.38	0.74	0.66	**19.0**	

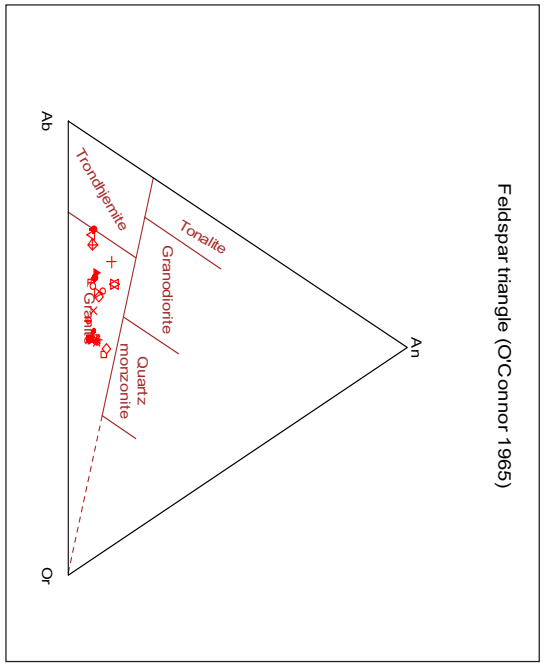

Fig.5. The An-Or –Ab diagram (fields after O'Connor, 1965) indicates that the granitoids are in the field of granitoid..

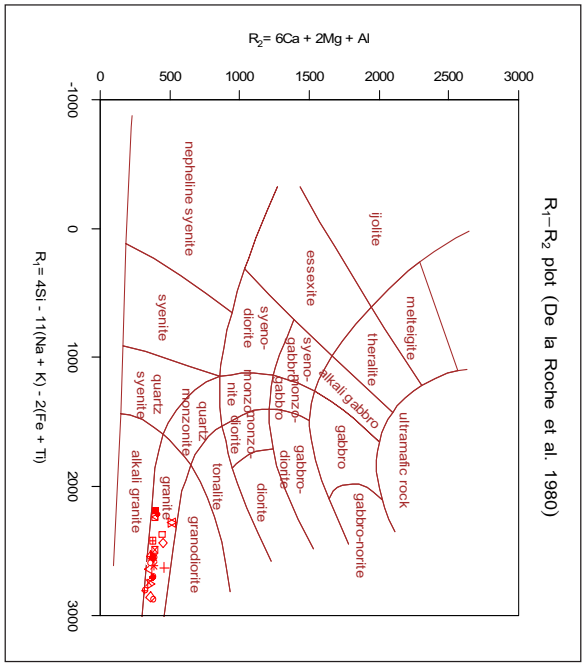

Fig.6. The R_1-R_2 diagram (fields after De La Roche et al., 1980) indicates that the granitoids are in granite field.

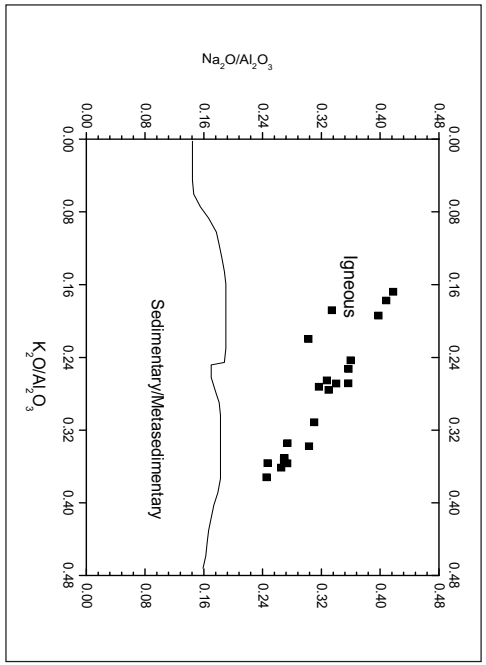

Fig.7. K_2O/Al_2O_3 vs. Na_2O/Al_2O_3 diagram (fields after Garrels& Mackenzie, 1971) indicates that the granitoids are in igneous field.

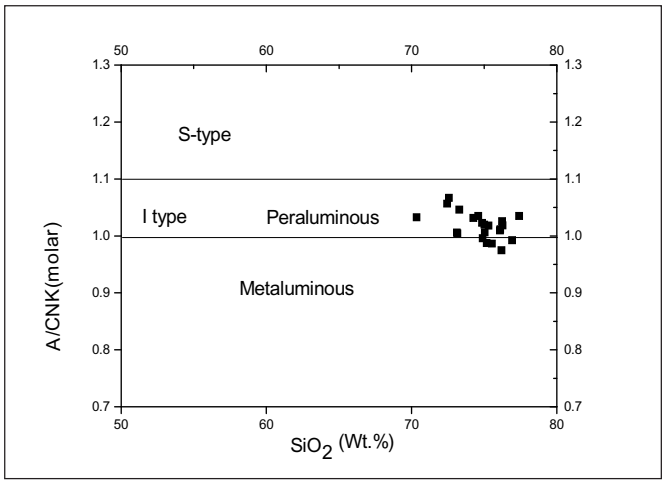

Fig..8. The SiO_2vs.A/CNK diagram (Fields after Chappell & White, 1974) indicates metaluminous to weakly peraluminous character of the granitoids.

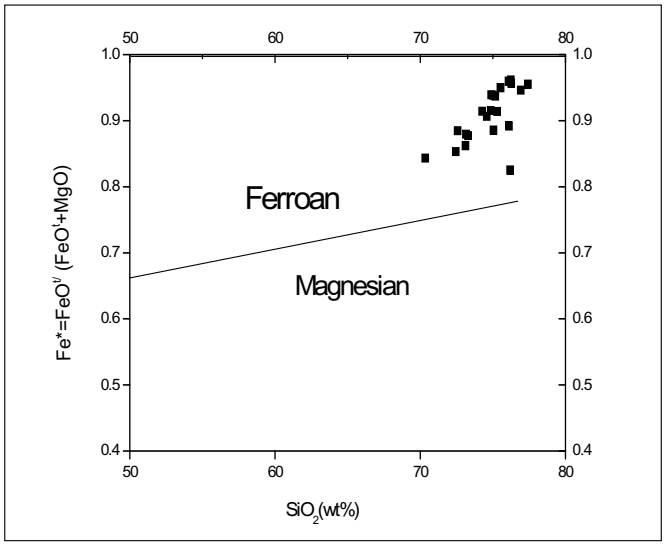

Fig.9. The SiO_2 vs. Fe* diagram for granitoids (Fields after Frost et al., 2001)

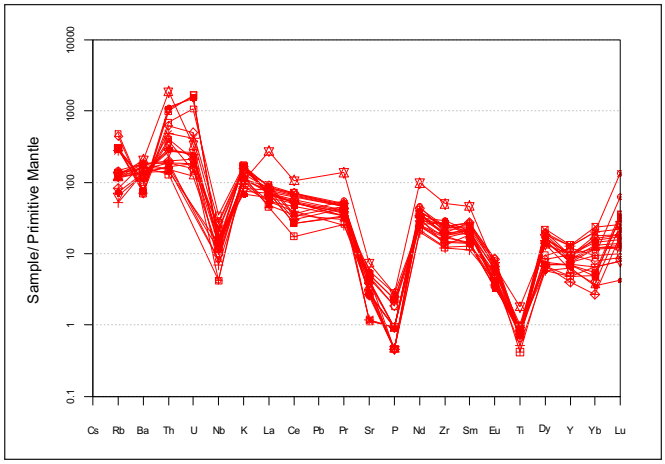

Fig.10. Primitive mantle normalised spider plot of the granitoids (values of normalisation after Sun and McDonough,1989) Ba, Nb, Sr, P, Ti, Yb showing depleted trend in this multi element diagram also indicating relative enrichment in Th, U, K.

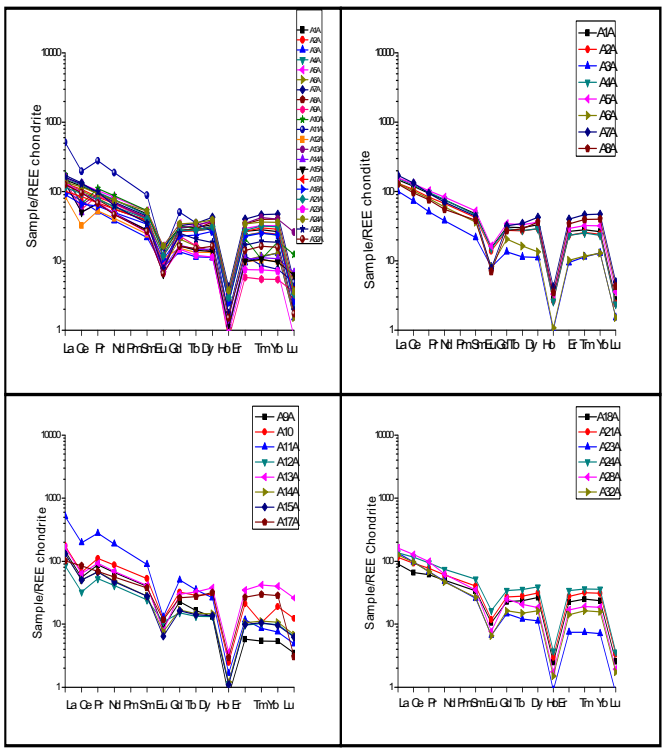

Fig.11. The Chondrite normalised REE pattern of the granitoids (normalisation values after Taylor and McLennan, 1985)

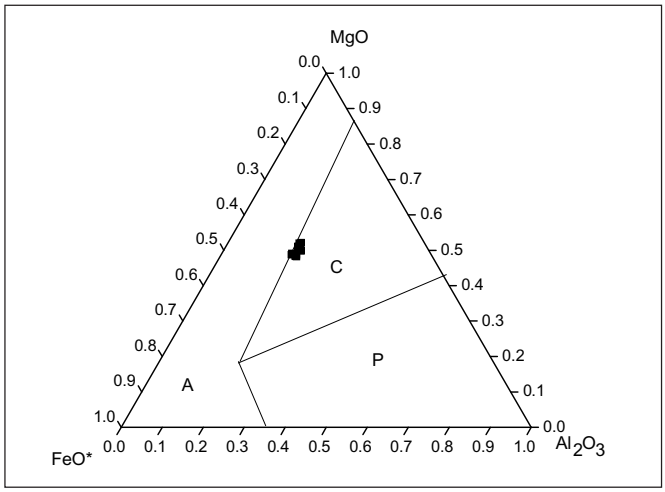

Fig.12. Biotites in the FeO*-MgO=Al_2O_3 triangular diagram (fields after Abdel-Rahman, 1994). A: alkaline, C: calc-alkaline, P: Peraluminous.

GEOTHERMOMETRY

Ti-in-Biotite Thermometer

TheTi-in biotite has been considered to be primarily a function of temperature and has been suggested as potential geothermometer (Engel and Engel, 1960; Kwak, 1968; Robert, 1976; Dymek, 1983). However, the Ti content in biotite is result of complex interplay among temperature, pressure, biotite crystal chemistry and coexisting mineral assemblages (Guidotti et al., 1977, 1988; Dymek, 1983; Labotka, 1983; Tracy and Robinson, 1988; Henry and Guidotti, 2002). Temperature effect appears to be most influential and the incorporation of Ti is relatively high at high temperatures, particularly higher than 800°C. Ti concentration decreases substantially with increase in pressure (Forbes and Flower, 1974; Robert, 1976; Arima and Edgar, 1981;

Table 4(a). EPMA data of biotite

Rock type	Granitoid													
	1 / 1	2 / 1	3 / 1	4 / 1	5 / 1	6 / 1	73 / 1	74 / 1	75 / 1	76 / 1	77 / 1	78 / 1	79 / 1	80 / 1
SiO_2	36.16	36.44	35.73	36.58	36.13	36.12	36.19	35.30	36.57	35.80	35.26	35.34	34.90	35.24
TiO_2	2.61	2.54	2.54	2.68	2.59	2.47	2.47	2.51	2.51	2.44	2.43	2.47	2.25	2.59
Al_2O_3	13.94	14.13	13.42	14.15	13.98	13.74	16.52	16.11	16.62	16.27	16.19	16.00	16.05	15.99
FeO	23.91	23.96	24.28	23.61	23.80	23.68	23.31	22.82	22.20	23.35	23.23	23.06	23.79	23.22
MnO	0.90	0.77	1.02	0.86	0.75	0.98	0.52	0.46	0.34	0.43	0.50	0.73	0.64	0.50
MgO	9.07	8.91	8.88	9.18	8.80	8.98	8.15	8.07	8.50	8.18	7.96	7.91	7.99	8.14
CaO	0.04	0.06	0.02	0.06	0.00	0.04	0.04	0.08	0.11	0.08	0.02	0.07	0.00	0.05
Na_2O	0.00	0.00	0.00	0.00	0.00	0.00	0.09	0.15	0.10	0.15	0.08	0.10	0.09	0.16
K_2O	9.30	9.34	9.59	9.55	9.55	9.40	9.66	9.43	9.64	9.34	9.41	9.48	9.38	9.47
Cl	0.14	0.12	0.13	0.12	0.15	0.13	0.03	0.04	0.03	0.05	0.04	0.04	0.05	0.05
F	0.75	0.66	0.69	0.62	0.63	0.67	0.00	0.08	0.08	0.05	0.04	0.04	0.00	0.09
Total	**96.83**	**96.92**	**96.29**	**97.41**	**96.37**	**96.21**	**96.99**	**95.06**	**96.70**	**96.14**	**95.16**	**95.23**	**95.13**	**95.49**
Number of ions on the basis of 11 oxygens														
Si	2.816	2.827	2.814	2.821	2.824	2.830	2.770	2.761	2.790	2.766	2.758	2.764	2.742	2.751
Al	1.279	1.292	1.246	1.286	1.288	1.269	1.490	1.485	1.494	1.482	1.492	1.475	1.486	1.471
"	4.095	4.119	4.060	4.107	4.112	4.099	4.260	4.256	4.284	4.248	4.250	4.239	4.228	4.222
Al	0.000	0.000	0.000	0.000	0.000	0.000	0.000	0.000	0.000	0.000	0.000	0.000	0.000	0.000
Ti	0.153	0.148	0.150	0.155	0.152	0.146	0.142	0.148	0.288	0.142	0.143	0.145	0.133	0.152
Fe(ii)	1.557	1.555	1.599	1.523	1.555	1.551	1.492	1.493	2.831	1.509	1.519	1.508	1.563	1.516
Mn	0.059	0.051	0.068	0.056	0.050	0.065	0.034	0.030	0.044	0.028	0.033	0.048	0.043	0.033
Mg	1.053	1.031	1.043	1.056	1.025	1.049	0.930	0.941	1.933	0.942	0.928	0.922	0.936	0.947
Ca	0.003	0.005	0.002	0.005	0.000	0.003	0.003	0.007	0.017	0.007	0.002	0.006	0.000	0.004
Na	0.000	0.000	0.000	0.000	0.000	0.000	0.013	0.023	0.028	0.022	0.012	0.015	0.014	0.024
K	0.924	0.924	0.964	0.940	0.952	0.939	0.943	0.941	1.875	0.921	0.939	0.946	0.940	0.943
Cl	0.018	0.016	0.017	0.016	0.020	0.017	0.004	0.005	0.008	0.007	0.005	0.005	0.007	0.007
F	0.185	0.162	0.172	0.151	0.156	0.166	0.000	0.020	0.039	0.012	0.010	0.010	0.000	0.022
Total	**7.844**	**7.833**	**7.886**	**7.842**	**7.846**	**7.852**	**7.819**	**7.828**	**7.794**	**7.819**	**7.826**	**7.831**	**7.856**	**7.842**
X_{Fe}	0.596	0.601	0.605	0.590	0.603	0.597	0.616	0.613	0.594	0.616	0.621	0.621	0.625	0.615
X_{Mg}	0.404	0.399	0.395	0.410	0.397	0.403	0.384	0.387	0.406	0.384	0.379	0.379	0.375	0.385

Table 4(b). Ti-in biotite geothermometric analyses of granitoids (based on Henry et al., 2005).

Sample No.	Data set point	Ti	X_{Mg}= (Mg/(Mg+Fe))	T°C	Average T°C	Std Dev.
S42C	1/1	0.306	0.404	652	648	5.4
	2/1	0.297	0.399	646		
	3/1	0.301	0.395	642		
	4/1	0.311	0.410	656		
	5/1	0.304	0.397	650		
	6/1	0.291	0.403	643		
S38C	73/1	0.285	0.384	637	642	6.4
	74/1	0.295	0.387	644		
	75/1	0.288	0.406	642		
	76/1	0.283	0.384	636		
	77/1	0.285	0.379	637		
	78/1	0.290	0.379	640		
	79/1	0.265	0.375	623		
	80/1	0.305	0.385	640		

Tronnes et al., 1985). Ti content in biotite increases with an increase in Fe content (Arima and Edgar, 1981; Abrecht and Hewitt, 1988) indicating compositional influence. Therefore, theTi content in biotite is result of combination of many parameters. It is difficult to apply experimental findings to range of P-T conditions, bulk compositions and mineral assemblages found in igneous and metamorphic rocks.

TheTi-in-Biotite (TIB) geothermometer of Henry et al. (2005) is based on the Ti-saturation surface of near-isobaric natural biotite data for peraluminous metapelites equilibrated at 4-6 kbar. Temperatures can be determined either by plotting Ti content of biotite and Mg/(Mg+Fe) values on the simple binary diagram or by calculating T from the expression:

$$T = ([\ln (Ti) - a - c\ (X_{Mg})^3] / b)^{0.333}$$

where, T is temperature in ºC, Ti is the apfu normalized to 22 oxygens, X_{Mg} is $Mg/(Mg+Fe^t)$, and the a, b and c parameters are given as a = -2.3594, b = 4.6482 x10 and c = -1.7283. This expression is valid in the range X_{Mg} = 0.275-1.0, Ti = 0.04-0.6 apfu and T = 480-800 ºC. Due to isotherm spacing, temperatures are more uncertain at low temperatures (< 600 ºC) than at high temperatures. Based on the standard deviations of the temperatures in our calibrated data set from the saturation surface, the uncertainty of the Ti-in-biotite geothermometer is estimated to be ±24ºC at lower temperatures (< 600ºC), improving to ±12 ºC at high temperature (>700 ºC) (Henry

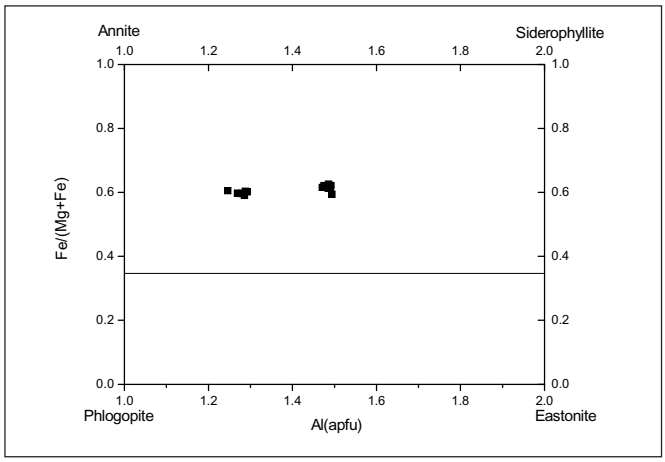

Fig.13. Biotites in the Annite – Siderophyllite – Phlogopite – Eastonite quadrilateral (fields after Speer, 1984).

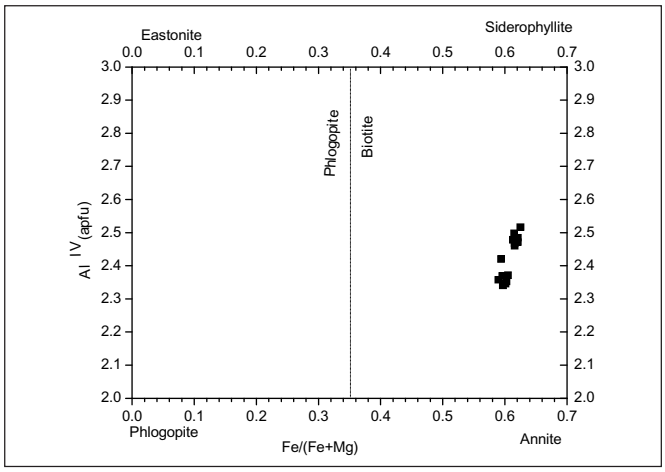

Fig.14. Biotites in the Fe/(Fe+Mg)vs.Al^{IV}diagram (fields after Deer et al., 1986).

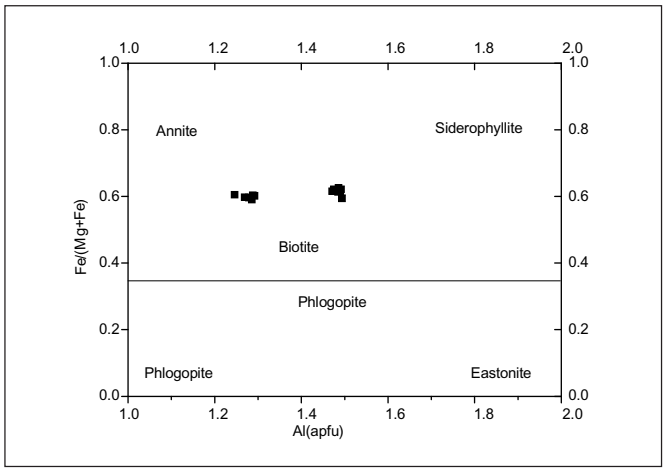

Fig.15. Biotites in the Al (apfu) vs. Fe/(Fe+Mg) diagram of Deer et al., 1986)

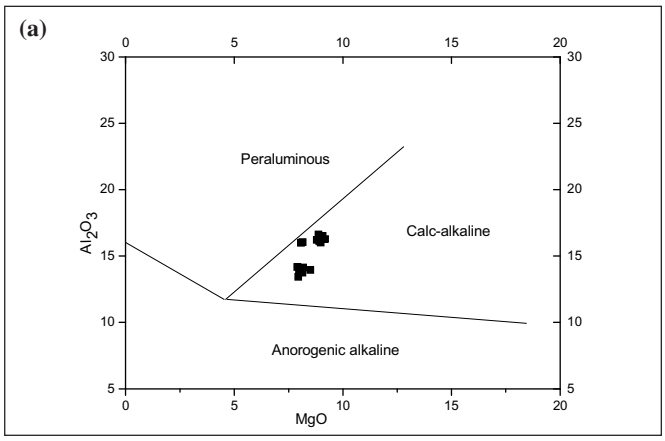

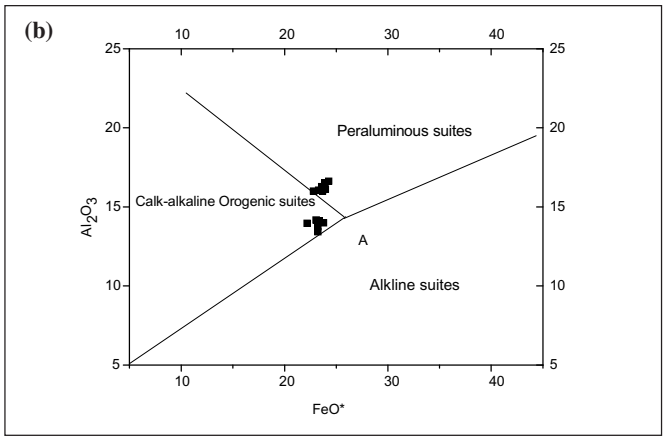

Fig.16. (a) Biotites in the MgO vs Al_2O_3 diagram. **(b)** Biotites in the FeO* vs. Al_2O_3 diagram (fields after Abdel-Rahman, 1994).

et al., 2005). The T values were calculated using Ti-in-biotite geothermometer software. The results are outlined in Table 4(b). The calculated range of temperature for granitoids is 623-656 ºC. The Ti-in biotite geothermometer of Henry et al. (2005) excel spreadsheet is used for the calculation.

However, theTi in biotite geothermometer of Henry et al. (2005) calibration data were metapelitic samples and valid only for biotite having mineral assemblages similar to those of calibration samples, fall within the range of biotite compositions, temperatures of the calibration samples and equilibrated roughly at 3.3 kbar. The accuracy of Ti-in biotite can be assessed if temperature estimate obtained by independent geothermometer or petrogenetic grids are available.

Two Feldspar Geothermometry

Natural feldspars are solid solutions of K-feldspar (Orthoclase, $KAlSi_3O_8$), Na-feldspar (Albite, $NaAlSi_3O_8$) and Ca-feldspar (Anorthite, $CaAl_2Si_2O_8$). The distribution of $NaAlSi_3O_8$ between two coexisting phases has been recognised as a valuable geothermometric tool (Barth, 1934, 1951). Two feldspar thermometry has had a long history of development. Early calibrations were based on binary exchange of albite component (e.g., Stromer, 1975; Whitney and Stromer, 1977; Heselton et al., 1983). Most recent offer three calibrations for each feldspar pair based on exchange of albite, anorthite and orthoclase components respectively (e.g., Ghiorso, 1984; Green and Usdansky, 1986; Elkins and Grove, 1990). Most thermometers are not sensitive to pressure, because the compositions of two co-existing feldspars in a rock strongly depend on temperature but less on pressure.In two feldspar thermometry, the feldspars are characterised by component exchanges easily reset during slow cooling or later thermal events;only in shallow emplaced plutons two feldspar thermometry yield consistent hyper solidusresults (Anderson, 2008).

The major element oxide values specially SiO_2, TiO_2, Al_2O_3, FeO(t), MnO, MgO, CaO, Na_2O, K_2O and Cr_2O_3 of plagioclase and alkali feldspars in granitoid rocks are plotted in a Multi-thermo-barometer Excel Calculation Sheet prepared by Putrika (2008), and T values obtained based on the equation given by Elkins and Groves (1990). The results are given in Table 5(c). The calculated range is 512-602°C.

DISCUSSION

Petrographic criteria such as presence of hornblende, biotite and sphene and absence of primary muscovite strongly suggests that the granitoids of the area are metaluminous, I-type granitoids (Whalen et al., 1987). The granitoids show distinct two feldspar mineralogy. This is possible only at higher water pressure, when the solvus and solidus curves intersect (subsolvus crystallisation) each other.

The granitoids have high SiO_2 content and contain more than 10% normative quartz. The normative corundum <1 wt%, normative diopside < 1 wt%, is in support of I-type nature of the granitoids. The Alumina Saturation Index (ASI) value indicates metaluminous to peraluminous character of the granitoids. The less than 1.1 molar A/CNK ratio suggests that granitoids are magmatic product with some crustal components.

The involvement of mantle and crust in the generation of granitoids can be seen in spider diagrams. The negative Nb anomaly, low contents

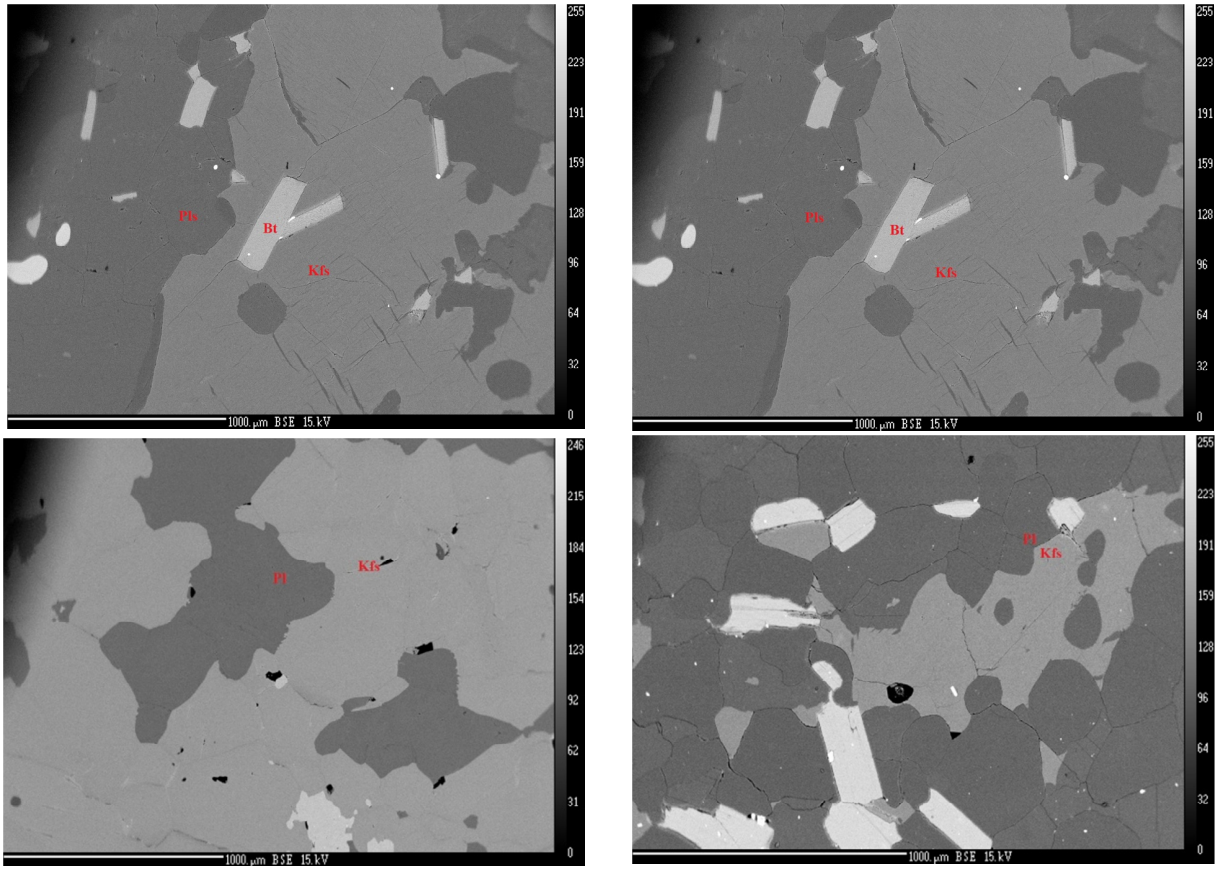

Fig.17. BSE images of granitoid. Pl = plagioclase, Kfs = potash feldspar, Bt = Biotite.

of Ti and P as displayed by multi element spider diagram, and also calc- alkaline nature is indication of subduction related origin. Therefore, the present granitoids produced from melting of mantle material and crustal material which were incorporated in subduction zone.

The REE pattern showing enrichment in both LREE and HREE, but enrichment of LREE relative to HREE is prominent. The REE pattern has negative anomaly at Eu. This type of REE pattern is characteristic of many Pan-African granitoids.

The biotites are identified as Annite-Siderophyllite from the discrimination plot. The biotites are calc-alkaline iron-rich in composition and have moderate to high aluminium content. Thus, the biotite mineral chemistry results are consistent with that of whole rock geochemistry.

The biotites are low in TiO_2 content and high in Al_2O_3 content. Oxygen fugacity (fO_2) can have profound influence on mineralogy and mineral composition of granitic rocks. So, it forms the foundation of magnetite versus ilmenite series granitic classification (Anderson, 2008). According to Ishihara (1977) ilmenite series granitoids were crystallised under oxygen reducing conditions in contrast to those magnetite series. Composition of biotite is very sensitive to temperature and oxygen fugacity. A low Ti content correlates with low temperature of crystallisation, low oxygen fugacity (Albuquerque, 1973; Buddington and Lindsley, 1964) and reflecting characteristics of ilmenite series of granitoids.

An attempt has been made to estimate the temperature existed during emplacement of rocks of the study area. For estimating the temperature of emplacement of granitic rocks two feldspar thermometer, Ti in biotite thermometer were used. Experimental studies have led to a view that granitic rocks will crystallise almost completely when cooled to 650-700^{0}C (Luth et al., 1964; Piwinskii et al., 1973; Tuttle et al., 1958). In the present study biotite crystals record crystallisation temperature from 623°C to 656°C (average is 645°C) and the temperature calculated from two feldspar thermometry is in the range 512-602°C (average 550°C). The calculated temperatures are near the accepted solidification temperature. The Ti content in the present granitoid is very low (vary from 0.13 to 0.29 apfu, average 0.29 apfu). The low Ti content in biotite demonstrates that these granitoids experienced low temperature of crystallisation. Low temperature biotite crystallisation is consistent with the temperature calculation based on composition of feldspars. However, the temperature of crystallisation of feldspar is below the accepted solidification temperature and also less than the biotite temperature. Many minerals in granitic rocks crystallise below 650°C (Glazner et al., 2013; Tuttle et al., 1948) and these low temperatures have commonly been interpreted as sub-solidus re-equilibration during hydrothermal alteration. The deduced temperature value (512-602°C) possibly corresponds to subsolvus feldspar equilibration with influence of higher P_{H2O}. Clouding of plagioclase, kaolinisation of alkali feldspar etc. are petrographic evidences in support of dominant control of P_{H2O}.

Different tectonic environments have characteristic geochemical signatures. Magma produced in different tectonic environment can be distinguished from one another on the basis of their geochemical characteristics. For the purpose the geochemical variation diagrams known as tectono-magmatic discrimination diagrams are used. On the Nb vs. Y diagram of Pearce et al. (1984) the granitoid plot mostly in VAG and syn-COLG field and in the Rb vs. (Y+Nb) diagram the granitoids mostly in the upper part of VAG field (Fig.18). On the tectonic SiO_2 vs. Rb/Zr discrimination diagram of Harris et al. (1986) the granitoids are in the field of volcanic arc and late or post collision settings (Fig.19). In the Al_2O_3 vs.Yb discrimination diagram the granitoids plot in the field of Low Al-TTG (oceanic field) (Fig.20). Accordingly, the granitoids have subduction related setting. The I-type leucocratic granitoid at subduction related setting (such as volcanic arc or late or post collision environments) can have wide

Table 5(a). EPMA data of K-feldspar

Rock Type	Granitoid																
	8 / 1	10 / 1	11 / 1	14 / 1	16 / 1	17 / 1	25 / 1	26 / 1	29 / 1	33 / 1	34 / 1	37 / 1	38 / 1	41 / 1	42 / 1	45 / 1	46 / 1
SiO_2	64.41	65.35	63.91	63.83	64.23	64.41	64.55	64.14	64.42	65.397	64.397	65.041	64.507	64.95	64.762	65.729	64.808
Al_2O_3	18.32	18.53	17.95	18.07	17.92	18.35	18.34	18.16	18.14	18.392	18.177	18.037	17.928	18.506	18.356	18.534	18.24
FeO	0.03	0.13	0.12	0.00	0.00	0.12	0.00	0.12	0.02	0.033	0	0.02	0	0.157	0.163	0	0.057
CaO	0.06	0.07	0.02	0.00	0.00	0.00	0.03	0.00	0.00	0.008	0	0.003	0.013	0.044	0	0	0
Na_2O	0.84	2.71	0.70	1.01	0.72	0.98	0.73	0.38	0.61	0.939	0.668	0.532	0.39	0.65	0.328	0.989	0.527
K_2O	15.63	12.65	15.88	15.61	15.59	15.42	15.64	15.60	15.75	15.113	15.667	15.752	15.653	15.569	15.628	15.136	15.803
BaO	0.33	0.32	0.24	0.27	0.21	0.25	0.26	0.31	0.24	0.344	0.173	0.237	0.279	0.308	0.302	0.25	0.341
Total	**99.62**	**99.76**	**98.81**	**98.79**	**98.66**	**99.53**	**99.55**	**98.70**	**99.17**	**100.226**	**99.082**	**99.622**	**98.77**	**100.184**	**99.539**	**100.638**	**99.776**
Number of ions on the basis of 8 oxygens																	
Si	2.992	2.997	2.997	2.992	3.007	2.992	2.996	3.002	3.002	3.006	3.002	3.014	3.015	2.995	3.003	3.006	3.003
Al	1.003	1.002	0.992	0.998	0.989	1.004	1.003	1.002	0.996	0.996	0.998	0.985	0.987	1.006	1.003	0.999	0.996
Σ	3.995	3.999	3.989	3.990	3.997	3.996	3.999	4.004	3.998	4.002	4.100	3.999	4.002	4.001	4.006	4.005	3.999
Fe(ii)	0.001	0.005	0.005	0.000	0.000	0.005	0.000	0.005	0.001	0.001	0.000	0.001	0.000	0.006	0.006	0.000	0.002
Ca	0.003	0.003	0.001	0.000	0.000	0.000	0.001	0.000	0.000	0.000	0.000	0.000	0.001	0.002	0.000	0.000	0.000
Na	0.075	0.241	0.064	0.092	0.065	0.088	0.066	0.034	0.055	0.084	0.241	0.048	0.035	0.058	0.029	0.088	0.047
K	0.926	0.740	0.950	0.933	0.931	0.914	0.926	0.931	0.936	0.886	3.726	0.931	0.933	0.916	0.924	0.883	0.934
Ba	0.006	0.006	0.004	0.005	0.004	0.005	0.005	0.006	0.004	0.006	0.013	0.004	0.005	0.006	0.005	0.004	0.006
Total	**5.007**	**4.993**	**5.013**	**5.021**	**4.996**	**5.007**	**4.998**	**4.980**	**4.995**	**4.980**	**19.980**	**4.983**	**4.976**	**4.989**	**4.972**	**4.980**	**4.989**
An (Mol%)	0.310	0.330	0.010	0.000	0.000	0.000	0.15	0.000	0.000	0.040	0.000	0.020	0.070	0.220	0.000	0.000	0.000
Ab (Mol%)	7.490	24.510	6.270	8.950	6.560	8.810	6.61	3.570	5.560	8.620	6.090	4.880	3.650	5.950	3.090	9.030	4.820
Or (Mol%)	92.200	75.160	93.630	91.050	93.440	91.190	93.24	96.430	94.440	91.330	93.910	95.100	96.290	93.820	96.910	90.970	95.180

Table 5(b). EPMA data of plagioclase

Rock Type	Granitoid																
Wt%	7 / 1	9 / 1	12 / 1	13 / 1	15 / 1	18 / 1	27 / 1	28 / 1	31 / 1	32 / 1	36 / 1	39 / 1	40 / 1	43 / 1	44 / 1	47 / 1	48 / 1
SiO_2	64.60	63.66	63.99	63.57	63.87	64.93	68.71	67.67	68.30	67.91	68.03	67.29	68.77	67.79	67.94	67.49	69.44
Al_2O_3	23.07	22.38	22.72	22.58	22.62	22.80	20.51	20.53	19.64	20.24	20.38	20.38	20.63	20.45	20.49	20.25	20.46
FeO	0.00	0.04	0.12	0.13	0.11	0.10	0.00	0.02	0.02	0.03	0.07	0.02	0.00	0.00	0.05	0.07	0.07
CaO	4.31	4.06	4.12	4.35	4.13	3.86	1.33	1.40	0.49	1.32	1.49	1.34	1.34	1.37	1.42	1.33	1.25
Na_2O	9.43	9.66	9.57	9.48	9.58	9.67	11.14	11.02	11.58	11.02	11.08	11.07	11.14	11.05	11.22	11.08	11.10
K_2O	0.24	0.20	0.27	0.18	0.25	0.20	0.21	0.19	0.16	0.19	0.12	0.18	0.23	0.21	0.21	0.15	0.12
BaO	0.02	0.05	0.00	0.00	0.00	0.02	0.00	0.00	0.00	0.01	0.05	0.00	0.00	0.00	0.00	0.00	0.08
Total	**101.66**	**100.05**	**100.78**	**100.28**	**100.56**	**101.58**	**101.90**	**100.84**	**100.18**	**100.73**	**101.22**	**100.28**	**102.11**	**100.87**	**101.33**	**100.38**	**102.54**
Number of ions on the basis of 8 oxygens																	
Si	2.810	2.817	2.811	2.808	2.812	2.825	2.995	2.943	2.983	2.995	2.949	2.943	2.952	2.947	2.943	2.949	2.966
Al	1.183	1.167	1.176	1.175	1.174	1.169	1.039	1.052	1.011	1.083	1.041	1.051	1.044	1.048	1.046	1.043	1.030
Σ	3.992	3.984	3.987	3.983	3.986	3.994	4.034	3.995	3.994	4.078	3.990	3.994	3.996	3.995	3.989	3.992	3.996
Fe(ii)	0.000	0.001	0.004	0.005	0.004	0.004	0.000	0.001	0.001	0.001	0.003	0.001	0.000	0.000	0.002	0.003	0.002
Ca	0.201	0.192	0.194	0.206	0.195	0.180	0.061	0.065	0.023	0.062	0.069	0.063	0.062	0.064	0.066	0.062	0.057
Na	0.975	0.829	0.815	0.812	0.818	0.816	0.929	0.929	0.980	0.930	0.931	0.939	0.927	0.931	0.942	0.939	0.919
K	0.013	0.011	0.015	0.010	0.014	0.011	0.012	0.011	0.009	0.011	0.007	0.010	0.013	0.012	0.012	0.008	0.007
Ba	0.000	0.001	0.000	0.000	0.000	0.000	0.000	0.000	0.000	0.000	0.001	0.000	0.000	0.000	0.000	0.000	0.001
Total	**5.003**	**5.019**	**5.016**	**5.016**	**5.017**	**5.004**	**5.036**	**5.001**	**5.007**	**4.996**	**5.000**	**5.006**	**4.998**	**5.001**	**5.011**	**5.003**	**4.982**
An (Mol%)	19.900	18.640	18.930	20.030	18.980	17.870	6.120	6.490	2.260	6.140	6.870	6.201	6.150	6.340	6.460	6.170	5.820
Ab (Mol%)	78.780	79.583	79.590	78.990	79.660	81.020	92.730	92.460	96.850	92.800	92.470	92.800	92.590	92.510	92.400	93.00	93.520
Or (Mol%)	1.320	1.456	1.480	0.990	1.370	1.100	1.150	1.050	0.880	1.050	0.660	0.990	1.260	1.160	1.140	0.830	0.670

Table 5(c). Two feldspar thermometry of granitoids

	K-feldspar-plagioclase	Temperature (°C)	Average T °C
S38C	25/1-28/1	519	538
	30/1-31/1	558	
	38/1-39/1	512	
	41/1-43/1	564	
S42C	10/1-9/1	602	563
	11/1-12/1	524	

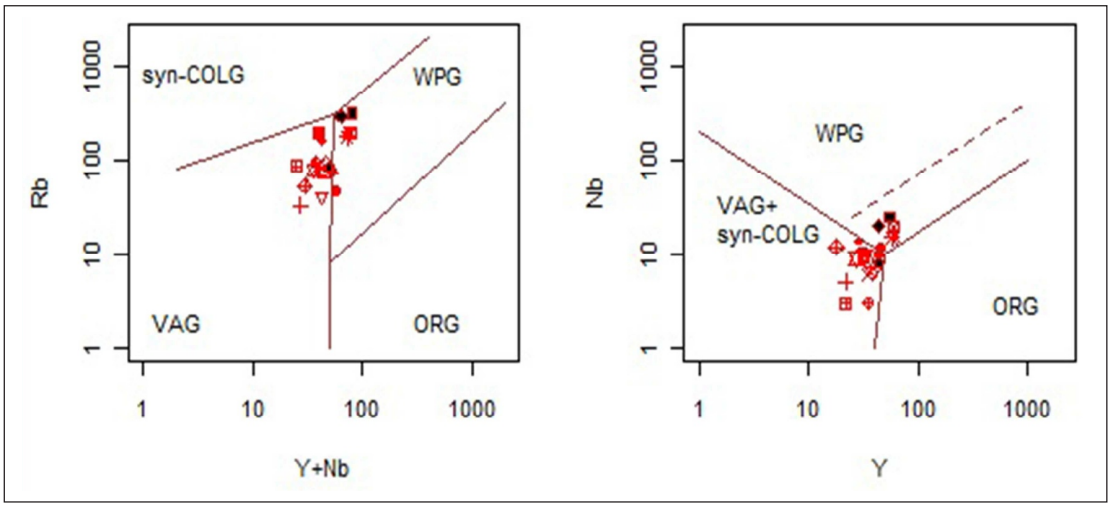

Fig.18. The Rb-(Y+Nb) and Nb-Y discrimination diagrams for the granites (fields after Pearce et al., 1984)

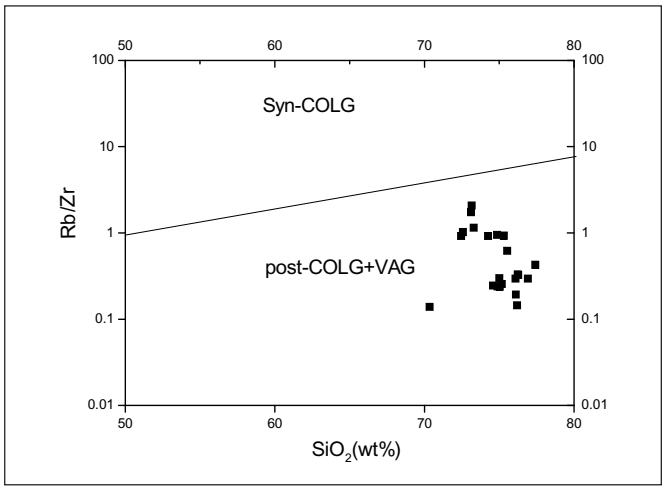

Fig.19. The granites in Rb/Zr vs.SiO_2 diagram (fields after Harris et al., 1986).

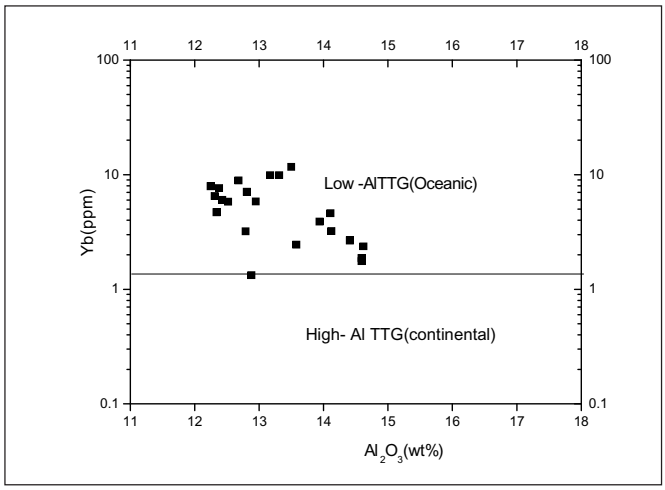

Fig.20. The Al_2O_3 vs. Yb value plot for diorite (fields after Arth, 1979).

range of sources (Sheppard et al., 2003). The calc-alkaline characteristic of the granitoid indicate the present granitoids may be the product of interaction between crustal and mantle derived components (Barbarin, 1999; Zhao and Zhou, 2009). The dehydration of the down going slab before melting release water and initiates partial melting. The hydrous minerals in subducting slab release their bound water into overlying hotter shallower mantle where melting begins. The buoyant hydrous magmas then ascend and encounter increasingly hotter surroundings (Condie, 2016)**.**

The different tectonic classification schemes indicated that the present granitoids were post-collisional and formed at subduction related tectonic settings. Geochemical study indicates that the present granitoid is highly fractionated I-type granitod.

The Pan-African magmatism in Shillong plateau is well established by several studies (Ghosh et al.,2005; Chatterjee et al.,2007,2011; Mazumdar and Dutta 2016; Kumar et al.,2017). I-type, highly fractionated, metaluminous to weakly peraluminous granitoids (in post collisional setting) linked to the Pan-African orogeny are described from Nongpoh and Mylliem plutons (Choudhury and Hussain, 2020) of Shillong Plateau.

CONCLUSION

This study brings out for the first time petrography and geochemical characters of the granitoids of the Jirang Patharkhamah area, Ri-Bhoi District Meghalaya. The present granitoid is metaluminous to weakly peraluminous nature and having I-type origin as revealed by petrographic study and geochemical plots. The tectonic classification studies indicated that the present granitoids are post-collisional and formed at subduction related tectonic settings. Studies reveal that the granitoids were product of dehydration melting of deep-seated meta igneous rocks in the subduction related tectonic environment. The biotite chemistry is in support of calc-alkaline, I-type nature of the granitoids. The temperature of crystallisation of magma is low. The tectonochemical signatures borne by the granitoids is characteristic of many Pan-African granitoids.

Acknowledgement: The present work is a part of Ph.D research work carried out by Anamika Gogoi at the Department of Geological Sciences, Gauhati University, Assam, India under the guidance of Dr. B. Bhagabaty.

References

Abdel-Rahman, A. (1994) Nature of biotites from Alkaline, calc-alkaline, and peraluminous magmas. Jour.Petrol., v.35(2), pp.525-541.

Abrecht, J. and Hewitt, D.A. (1988) Experimental evidence on the substitution of Ti in biotite. Amer. Mineral., v.73, pp.1275-1284.

Ague, J.J., Brimhall, G.H. (1988) Regional variations in bulk chemistry, mineralogy, and compositions of mafic and accessory minerals in batholiths of California. Geol. Soc. Amer., v.100(6), pp.891-911.

Albuquerque, C.A. (1973) Geochemistry of biotites form granitic rocks, Northern Portugal. Geochim. Cosmochim. Acta, v.37, pp.1779-1802.

Anderson, J.L., Barth, A.P, Young, E.D. (1988) Mid-crustal Creteceous roots of Cordilleran metamorphic core complexes. Geology, v.16(4), pp.366-369.

Anderson, J.L., Barth, A.P., Wooden, J.L., Mazab, F. (2008) Thermometers and Thermobarometers in Granitic Systems. Rev. Mineral. Geochem., v.69(1), pp.121-142.

Arima, M. and Edgar, A.D. (1981) Substitution mechanisms and solubility of titanium in phlogopites from rocks of probable mantle origin. Contrib. Mineral. Petrol., v.77, pp.288-295.

Arth, J.G. (1979) Some trace elements in Trondhjemite-their implications to magma genesis and paleotectonic setting. *In:* F. Barker (Ed.), Trondhjemites, Dacites and Related rocks.: Amsterdam, Elsevier Scientific Publishing Co., pp.1-12.

Barbarin, B. (1999) A review of relationships between granitoid types, their origins and their geodynamic environments. Lithos, v.46, pp.605-626.

Barth, T.F.W. (1934) Polymorphic phenomena and crystal structure. Amer. Jour. Sci., v.5, pp.273.

Barth, T.F.W. (1951) The feldspar geological thermometers. Neues Jahrb. Mineral, v.82, pp.143-154.

Bhagabaty, B. and Mazumdar, A.C. (2008) Petrology of granulites from Shillong Plateau in West Garo Hills district, Meghalaya, India. Jour. Nepal Geol. Soc., v.37, pp.1-10.

Bhagabaty, B., Mazumdar, A.C. and Borah, P. (2017) Geochemical characteristics of Tukureswari and Barbhita Granitoids in Goalpara District,Assam. Jour. Geol. Soc. India, v.89, pp.532-540.

Bidyanand, M. and Deomurari, M.P. (2007) Geochronological constraints on the evidence of Meghalaya massif, northeastern India: an ion microprobe study. Curr. Sci., v.93(11), pp.1620-1623.

Buddington, A.F., Lindsley, D.H. (1964) Iron-titanium oxide minerals and synthetic equivalents. Jour. Petrol., v.5, pp.310-357.

Burkhand, D.J.M. (1993) Biotite crystallisation temperature and redox states in granitic rocks as indicator for tectonic setting. Geol. Mijnbouw, v.71, pp.337-349.

Chappell, B.W. and White, A.J.R. (1974) Two contrasting granite types. Pacific Geol., v.8, pp.173-174.

Chattejee, N., Mazumdar, A.C., Bhattacharya, A. and Siakia, R.R. (2002) Neoproterozoic highly fractionated I-type granitoids of Shillong Plateau, Meghalaya, Northeast India: geochemical constraints on their petrogenesis. Acta Geochim., v.40, pp.51-66.

Chatterjee, N., Bhattacharya, A., Duarah, B. P. and Mazumdar, A. C. (2011) Late Cambrian Reworking of Paleo-Mesoproterozoic Granulites in Shillong-Meghalaya Gneissic Complex (Northeast India): Evidence from PT Pseudosection Analysis and Monazite Chronology and Implications for East Gondwana Assembly. Jour. Geol., v.119(3), pp.311-330.

Clarke, D.B., Dorais, M., Barbarin, B., Barker, D., Cesare, B., Clarke, G., El Baghdadi Erdmann, S., Forster, H.J., Gaeta, M., Gottesmann, B., Jamieson, R. A., Kontak, D. J., Koller, F., Gomes, C. L., London, D., Morgan V I. G. B. Neves, L.J.P. F., Pattison, D.R.M., Pereira, Pichavant, M., Rapela, C.W., Renno,A. D., Richards, S., Roberts, M., Rottura, A., Saavedra, J., Sial, A.N., Toselli, A.J., Ugidos, J.M., Uher, P., Villaseca, C., Visona, D., Whitney, D. L., Williamson, B., and Woodard, H.H. (2005) Occurrence and origin of andalusite in peraluminous felsic igneous rocks. Jour. Petrol., v.46, pp.441-472.

Condie, K.C. (2016) Earth as an evolving planetary system; 3rd ed., 430p.

Dahlquist, J.A., Galindo, C., Pankhurst, R.J., Rapela, C.W., Alsino, P.H., Saavedra, J. and Fanning, C.M. (2007) Magmatic evolution of the Penon Rosado Granite: petrogenesis of garnet bearing granitoids. Lithos, v.95, pp.177-207.

Dash, C.R. and Chatterjee, B. (1992) Geology of the Patharkhammah-Umpyrtha, East Khasi Hills district, Meghalaya. Geol. Surv. India Publ. v.125(4), pp.24-26.

De La Roche, H., Leterrier, J., Grandelaude, P. and Marchal, M. (1980) A classification of volcanic and plutonic rocks using R1R2-diagram and major element analyses-Its relation with current nomenclature. Chemical Geol., v.29(1-4), pp.183-210.

Deer, W.A., Howie, A. and Zussman, J. (1986) An introduction to rock-forming minerals. 17th Longman Ltd., v.528, pp.16.

Dodge, F.C.W., Smith, V.C. and Mays, R.E. (1969) Biotite from granitic rocks of the central Sierra Nevada batholiths, California. Jour. Petrol., v.120, pp.250-271.

Dwivedi, S.B. and Theunuo, K. (2011) Two pyroxene bearing Granulites from Patharkhang Shillong –Meghalaya Gneissic Complex (SMGC). Curr. Sci., v.100, pp.100-105.

Dymek, R.F.(1983) Titanium, aluminium and interlayer cation substitutions in biotite from high grade gneisses,West Greenland. Amer. Mineral.,v .68, pp.880-899.

Egal, E., Thieblemont, D., Lahondere, D., Guerrot, C., Costea, C.A., lliescu, D., Delor, C., Goujou, J.C., Lafon, J.M., Tegyey, M., Diabyand, S. and Kolie, P. (2002) Late Eburnean granitization and tectonics along the western and north western margin of the Archean Kenema-Man domain (Guinea,West African Craton). Precambrian Res., v.117, pp.57-84.

Elkins, L.T. and Grove, T.L. (1990) Ternary feldspar experiments and thermodynamic models. Amer. Mineral., v.75, pp.544-559.

Evans, P. (1964) The tectonic framework of Assam. Jour. Geol. Soc. India, v.5, pp.80-96.

Finch, A.A., Parsons, I. and Mingard, S.C.(1995) Biotite as indicator of fluorine fugacities in late stage magmatic fluids: the Garder province of south Greenland. Jour. Petrol., v.36(6), pp.1701-1728.

Forbes, W.C. and Flower, M.F.J.(1974) Phase relations of titan-phlogopite $K_2Mg_4TiAl_2Si_6O_{20}(OH)_4$: a refractory phase in the upper mantle? Earth Planet. Sci. Lett., v.22(1), pp.60-66.

Frost, B.R., Barnes, C.G., Collins, W.J., Arculus, R.J., Ellis, D.J. and Frost, C.D. (2001) A geochemical classification for granitic rocks. Jour. Petrol., v.42, pp.2033-2048.

Garrels, R.M. and Mackenzie, F.T. (1971) Evolution of Sedimentary rocks, W.W. Norton & Co., New York, 394p.

Ghiroso, M.S. (1984) Activity/composition relations in the ternary feldspar. Contrib. Mineral. Petrol., v.87(3), pp.282-296.

Ghosh, S., Chakraborty, S., Bhalla J.K., Paul, D.K., Sarkar, A., Bishui, P.K. and Gupta, S.N. (1991) Geochronology and geochemistry of granite plutons from East Khasi Hills, Meghalaya. Jour. Geol. Soc. India, v.37, pp.331-342.

Ghosh, S., Chakraborty, S., Paul, D.K., Bhalla, J.K., Bishui, P.K. and Gupta, S.N. (1994a) New Rb-Sr isotopic ages and geochemistry of granitoids from Meghalaya and their significance in middle to late Proterozoic crustal evolution. Indian Minerals, v.48, pp.33-44.

Ghosh, S., Fallic, A.E., Paul, D.K. and Potts, P.J. (2005) Geochemistry and origin of Neoproterozoic granitoids of Meghalaya, Northeast India: Implicatins for linkage with amalgamation of Gondwana supercontinent. Gondwana Res., v.8, pp.421-432.

Glazner, A.F. and Johnson, B.R. (2013) Late crystallisation of K-feldspar and the paradox of megacystis granites. Contrib. Mineral. Petrol., v.166, pp.777-799.

Guidotti, C.V., Cheney, J.T. and Guggenheim, S. (1977) Distribution of Ti between coexisting phases between muscovite and biotite in politic schists of northwestern Maine. Amer. Mineral., v.62, pp.438-448.

Guidotti, C.V., Cheney, J. and Henry, D.J. (1988) Compositional variation of biotite as a function of metamorphic reactions and mineral assemblage in the politic schists of western Maine. Amer. Jour. Sci., v.288, pp.270-292.

Harris N.B.W., Pearce, J.A. and Tindle, A.G. (1986). Geochemical characteristics of collision zone magmatism.-In: Coward, M.P. & Ries, A.C.(Eds);Collision tectonics –Geol. Soc. Lond. Spec. Publ. v. 9, pp. 67-81.

Henry, D.J., Guidotti, C.V. and Thomson, J.A. (2005) The Ti saturation surface for low to medium pressure metapelitic biotite: Implications for geothermometry and Ti substitution mechanism. Amer. Mineral., v.90, pp.316-328.

Henry, D.J. and Guidotti,C.V. (2002) Ti in biotite from metapelitic rocks: Temperature effects,crystallochemical controls and petrologic application. Amer. Mineral., v.87, pp.375-382.

Heselton, H.T., Jr., Hovis, G.L., Hemmingway, B.S., Robie, R.A. (1983) Calorimetric investigation of excess entropy of mixing in albite –sanidine solid solutions:lack of evidence for Na, K short range order and implications for two feldspar thermometry. Amer. Mineral., v.68, pp.398-413.

Ishihara, S. (1977) The magnetite series and ilmenite series granitic rocks. Mining Geol., v.27, pp.293-305.

Ishihara, S. (1981) The granitoid series and mineralization. Econ. Geol., 75th Anniver. volume, pp.458-484.

Kemp, A.I.S., Hawkesworth, C.J., Foster, G.L., Paterson, B.A., Woodhead, J.D., Hergt, J.M., Cray, C.M., Whitehouse, M.J. (2007). Magmatic and crustal differentiation history of granitic rocks from Hf-O isotopes in zircon. Science, v.315(5814), pp.980-983.

Kumar, S. (1990) Petrochemistry and geochronology of pink granite from Songsak, East Garo Hills, Meghalaya. Jour. Geol. Soc. India, v.35, pp.277-279.

Kumar, S. (1998) Granitoids and their enclaves from east Khasi hills of Meghalaya: Petrogenetic and Geochemical reappraisal. Workshop on "Geodynamics and Natural Resources of North East India. Dibrugarh, Assam, Abstract volume, pp.17-18.

Kumar, S. (2009) Geology of North –east India: Frontiers for Research Activities. *In:* M.K. Mazumdar (Ed.), Geoscientific Issues of North-east India, Pragjyotish College, Guwahati, pp.103-111.

Kumar, S. Pieru, T., Rino, V. and Lyngooh, B.C. (2005) Microgranular enclaves in Neoproterozoiv granitoids of South Khasi Hills, Meghalaya Plateau, North East India; field evidences of interacting coeval mafic and felsic magmas. Jour. Geol. Soc. India, v.65, pp.629-633.

Kumar, S., Rino,V., Hayasaka, Y., Kimura, K., Raju, S., Terada, K. and Pathak, M. (2017) Contribution of Columbia and Gondwana Supercontinent assembly and growth related magmatism in the evolution of Meghalaya Plateau and Mikir Hills, Northeast India: constraints from U-PbSHRIMP zircon geochronology and geochemistry. Lithos, v.277, pp.356-377.

Labotka, T. C. (1983) Analysis of the compositional variations of biotite in politic hornfels from northeastern Minnesota. Amer. Mineral., v.68, pp.900-914.

Lal, R.K., Ackermand, D., Scifert, F. and Halder, S.K. (1978) Chemographic relationship in Sapphirine bearing rocks from Sonapahar, Assam, India. Mineral. Petrol., v.67, pp.169-187.

Luth,W.C., Jahns, R.H. and Tuttle, O.F. (1964) The granite system at pressures of 4 to 10 Kilo bars. Jour. Geophys. Res., v.69, pp.759-773.

Majumdar, D. and Dutta, P. (2016) Geodynamic evolution of a Pan-African granitoid of extended Dizo Valley in Karbi Hills, NE India: Evidence from Geochemistry and Isotope Geology. Jour. Asian Earth Sci., v.117, pp.256–268.

Mazumdar, S.K. (1976) A summary of the Precambrian Geology of Khasi Hills, Meghalaya. Geol. Surv. India Misc. Publ., v.23(2), pp.311-334.

Mazumdar, S.K. (1986) The Precambrian framework of part of the Khasi Hills, Meghalaya. Rec. Geol. Surv. India, v.117, pp.1-59.

Mitra, S.K. (1998) Structure, sulphide mineralization and age of the Shillong group of rocks, Meghalaya. Abst. volume, M.S. Krishnan Commem. Nat. Sem., pp.118-119.

Mitra, S.K. (2005) Tectonic setting of the Meghalaya Plateau and it's sulphide mineralization. Jour. Geol. Soc. India, v.65, pp.117-118.

Nachit, H., Razafimahefa, N., Stussi, J.M. and Caron, J.P. (1985) Composition chimique des Biotites et typologie magmatique des granitoids. C.R. Acad. Sci. Paris. Sr.II, v.301, pp.813-818.

Nandy, D.R. (2001) Geodynamics of northeastern India and the adjoining region. ABC Publication, Kolkata. 209p.

Neiva, A.M.R. (1981) Geochemistry of hybrid granitoid rocks and of their biotites from central northern Portugal and their petrogenesis. Lithos, v.14(2), pp.149-163.

O'Connor, J.T. (1965) A classification for quartz-rich igneous rock based on feldspar ratios. USGS Prof. Paper, 525B, B79-B84.

Pearce, J.A., Harris, N.B.W. and Tindle, A.G. (1984) Trace element discrimination diagrams for the tectonic interpretation of granitic rocks. Jour. Petrol., v.25(4), pp.956-983.

Piwinski, A.J. (1973) Experimental studies of granitoids from the Central and Southern Coast Ranges, California. Tchermaks Mineral. Petrogr. Mitt., v.20, pp.107-130.

Putrika, K., Tepley, F. (Eds.) (2008) Minerals, Inclusions and Volcanic Processes, Rev. Min. Geochem., Mineralogical Soc. Amer., v.69, pp. 61-120.

Ray, J., Saha, A., Ganguly, S., Balaram, V., Khishna, A.K. and Hazara, S. (2011) Geochemistry and Petrogenesis of Neoproterozoic Mylliem granitoids, Meghalaya Plateau, Northeastern India. Jour. Earth System Sci., v.120, pp.459-473.

Shabani, A., Lalonde, A.E., Whalen, J.B. (2003) Composition of biotite from granitic rocks of the Canadian Appalachian Orogen:A potential tectonomagmatic indicator? Canadian Mineral., v.41(6), pp.1381-1396.

Sheppard, S., Occipinti, S.A. and Taylor, I.M. (2003) The relationship between tectonism and composition of granitoid magmas, Yarlarweelor Gneiss complex, western Australlia. Lithos, v.66, pp.133-154.

Spear, J.A. (1981a) Petrology of cordierite and almandine bearing granitoid plutons of the southern Appalachian Piedmont. U.S.A. Canadian Mineral., v.19, pp.35-46.

Speer, J.A. (1984) Micas in Igneous Rocks, *In:* S.W. Bailey (Ed.), Micas: Reviews in Mineralogy. Mineral. Soc. Amer., v.13, pp.299-356.

Srivastava, R.K., Heman, L.M., Sinha, A.K., Shihua, S. (2004) Empalcement age and isotope geochemistry of Sung Valley alkaline-carbonatite complex, Shillong Plateau, northeastern India: Implications for primary carbonate melt and genesis of the associated silicate rocks. Lithos, v.81, pp.33-34.

Stormer, J.C., Jr. (1975) A Practical two –feldspar Geothermometer. Amer. Mineral., v.60, pp.667-674.

Sun, S.S. and McDonough, W.F. (1989) Chemical and isotope systematics of oceanic basalts: implication for mantle composition and processes. Geol. Soc. London Spec. Publ., v.42, pp.313-345.

Taylor, S.R. and McLennan, S.M. (1985) The continental crust:its composition and evolution. Blackwell Scientfic publication, Carlton, 312p.

Tonnes, R.G., Edgar, A.D. and Arima, M. (1985) A high pressure –high temperature study of TiO_2 solubility in Mg rich phlogopite:implications to phlogopite chemistry. Geochim. Cosmochim. Acta, v.49, pp.2323-2329.

Tracy, R.J., Robinson, P. (1988) Silicate-Sulfide-Oxide-fluid reaction in granulite grade politic rocks,Central Massachusetts. Amer. Jour. Sci., v.288A, pp.45-74.

Tuttle, O.F. and Friedman, I. (1948) Liquid immiscibility in the system H_2O-Na_2O-SiO_2. Amer. Chem. Soc. Jour., v.70, pp.919-926.

Tuttle, O.F., Bowen,N.L. (1958) Origin of granite in the light of experimental studies in the system $NaAlSi_3O_8$-$KAlSi_3O_8$-SiO_2-H_2O. Jour. Geol. Soc. Amer., v.74, pp.1-146.

Whalen, J.B., Currie, K.L. and Chappell, B.W. (1987) A type granites: geochemical characteristics, discrimination and petrogenesis. Contrib. Mineral. Petrol., v.95, pp.407-419

Whitney, J.A., Stromer,J.C. (1977) Two-feldspar geothermometry, geobarometry in mesozonal granitic intrusions: Three examples from the Piedmont of Georgia. Contrib. Mineral. Petrol., v.63(1), pp.51-64.

Wones, D.R. and Eugster, H.P. (1965) Stability of biotite experiment theory and applications. Amer. Mineral., v.59(9), pp.1228.

Yin, A., Dubey, C.S., Webb, A.A., Grove, M., Gehrels, G.E. and Burgess, W.P. (2010a) Geologic correlation of the Himalayan orogeny and Indian craton (part I): Structural Geology, U-Pb zircon Geochronology and Tectonic Evolution of the Shillong Plateau and its Neighbouring Regions in NE India. Bull. Geol. Soc. Amer., v.122 (3/4), pp.336-359.

Zhao, J.H. and Zhou, M.F. (2009) Melting of newly formed mafic crust for the formation of Neoproterozoic I-type granite in the Hannan region, South China. Jour. Geol., v.117, pp.54-70.